The Production of Copper–Arsenic Alloys (Arsenic Bronze) by Cosmelting: Modern Experiment, Ancient Practice

Heather Lechtman

*Center for Archaeological Materials, Department of Materials Science and Engineering,
Massachusetts Institute of Technology, Cambridge, MA 02139, U.S.A.*

Sabine Klein

Institut für Mineralogie, J.W. Goethe Universität, Senckenberganlage 28, D-60054 Frankfurt, Germany

Cosmelting experiments to produce copper–arsenic alloys were carried out by Lechtman in 1984. The experiments included crucible and furnace smelting techniques utilizing ores collected in the Peruvian Andes. Smelting charges consisted of mixtures of copper oxide ore with either copper sulpharsenide or iron sulpharsenide ore. The experimental furnaces were constructed to resemble furnaces excavated at Batán Grande, a large ore smelting site on the Peruvian north coast where copper–arsenic alloys were produced during the Middle Horizon and later.

The cosmelting experiments yielded coherent copper–arsenic alloy ingots over a wide range of oxide: sulpharsenide ore mixtures. Crucible/furnace charges containing ratios of between 2:1 and 4:1 oxide:sulpharsenide mineral produced clean metal, fully separated from slag or matte byproducts. The sulphide ores were not roasted prior to smelting; no flux was added to the charges.

Study of the metal ingots, mattes, and slags helps determine the chemical and thermodynamic reactions and the phase separation mechanisms that took place inside the smelting enclosures. The copper–arsenic alloys found in ancient artefacts could have been made easily, deliberately or accidentally, by cosmelting procedures. © 1999 Academic Press

Keywords: ARSENIC BRONZE, BRONZE PRODUCTION, COSMELTING, COPPER–ARSENIC ALLOYS.

Introduction

Alloys of copper and arsenic, some of which are referred to as arsenic bronze, were produced and used throughout the Near East and Europe from the early 4th millennium BCE to the Late Bronze Age (Heskel & Lamberg-Karlovsky, 1980; Muhly, 1988). The manufacture of arsenic bronze preceded the development of tin bronze in the Near East by more than a millennium, but the tin variety completely replaced the arsenic alloy by about 1500 BCE. In the Americas, arsenic bronze was first developed in the Andean zone of South America (Lechtman, 1979, 1996, 1997). It was one of the key alloys used throughout the central Andean region from the Middle Horizon until the end of the Late Intermediate Period (roughly CE 800–1450). The Inka preferred tin bronze, and after about CE 1450 bronze objects associated with the Inka hegemony tended to be made of the copper–tin alloy.

In spite of the predominance of arsenic bronze over long periods of time in two of the foremost ancient centres of metallurgical development, the Near East and the Andes, we remain uncertain about how the alloy was made. Archaeologists have analysed large numbers of artefacts fashioned from the material, but smelting sites where we can study the extractive technologies used to produce arsenic bronze are extremely rare.

The purpose of the investigation reported here was to test through experiment the feasibility of smelting oxide ores of copper together with arsenic-bearing sulphide ores (sulpharsenides) of either copper or iron to produce copper–arsenic alloys. Such extractive metallurgical procedures, in which the smelting charge is made up of a mixture of oxide and sulphide ores, are known as cosmelting. A primary consideration was to evaluate whether cosmelting technologies might have been used in the central Andean zone during the period when the volume of arsenic bronze production there was highest. Lechtman (1985) designed cosmelting experiments to utilize ores she had collected from Peruvian deposits and mines (Lechtman, 1976) and that represented ore types readily available to miners in prehistory. She built a series of smelting furnaces to resemble those excavated at Batán Grande, a
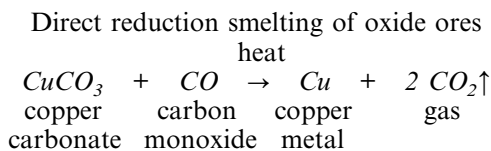
near-industrial smelting site on Peru's far north coast that produced large quantitites of arsenic bronze from about CE 900 to 1450 (Epstein & Shimada, 1983; Shimada & Merkel, 1991). All the experiments utilized Peruvian ores cosmelted in Batán Grande-type furnaces or in crucibles. In 1996–1997, during a post-doctoral residency at MIT, Sabine Klein analysed and interpreted the mineral and glassy phases present in the cosmelted products, including metal, matte, speiss, and slag, using X-ray diffraction and electron microanalytical methods.

## Metal Extraction by Direct Reduction Smelting or by Cosmelting

Until the advent of industrial methods for chemically separating metal from ore concentrates, extractive metallurgy—the winning of metal from metallic ores—was synonymous with ore smelting. The smelting techniques used to extract the metallic portion of an ore depend largely on the nature of the metallic mineral comprising the ore. Primary ore minerals are usually metallic sulphides; secondary ore minerals, metallic oxides, are the weathered, alteration products of the sulphides. There is ample evidence from many parts of the world demonstrating that the earliest smelting technologies usually involved winning copper metal from copper oxide ores. Copper "oxides" include the carbonate, sulphate, and chloride ores of copper.

Direct reduction

Direct reduction smelting, carried out in a simple furnace or crucible, is sufficient to win metallic copper from its oxide ores. The smelting enclosure must contain a reducing environment, provided by the partial burning of charcoal to carbon monoxide (CO). The monoxide combines with oxygen in the ore mineral, reducing the ore to its metallic component. The following equations are generalized examples of direct smelting reactions that occur inside a furnace or crucible; they are balanced, but the mineral formulae do not represent stoichiometric compounds.
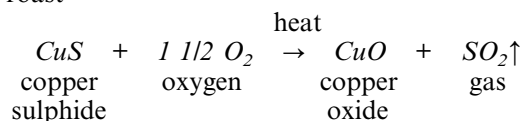
Direct reduction smelting of oxide ores

$$CuCO_3 \;+\; CO \;\xrightarrow{heat}\; Cu \;+\; 2\,CO_2\uparrow$$
copper   carbon   copper   gas
carbonate   monoxide   metal

If the metallic mineral in the ore is a copper arsenate (e.g., olivenite: $[Cu_2(AsO_4)(OH)]$), formed upon the weathering of a copper sulpharsenide ore (e.g., enargite: Cu_3AsS_4), direct reduction smelting of the oxide ore produces an alloy of copper and arsenic, the two metallic components of the ore mineral.

$$CuAsO_4 \;+\; 4\,CO \;\xrightarrow{heat}\; Cu,As \;+\; 4\,CO_2\uparrow$$
copper   Cu-As
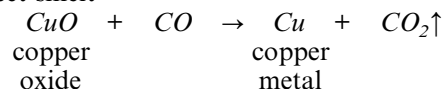arsenate   alloy
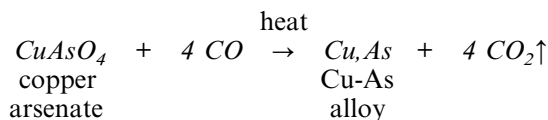
Most of the world's arsenic-bearing ores are sulphides. The Andean region, for example, is particularly rich in sulpharsenide ores of copper, such as enargite. The sulpharsenide ore of iron, arsenopyrite (FeAsS), is also present in the Andes though much less abundantly. Sulphide ores cannot be reduced by carbon monoxide. This fact led many investigators (see, e.g., Charles, 1980; Tylecote, 1980b; Zwicker et al., 1985; Rapp, 1989) to assume that the only option available to early metalworkers for extracting metal from sulphide ores was to follow a two-step process: (1) roast the ore to drive off the sulphur as sulphur dioxide gas; (2) follow the roast by a direct smelt of the oxide ore produced during roasting.

Roasting sulphide ore, followed by direct smelting of the oxide product
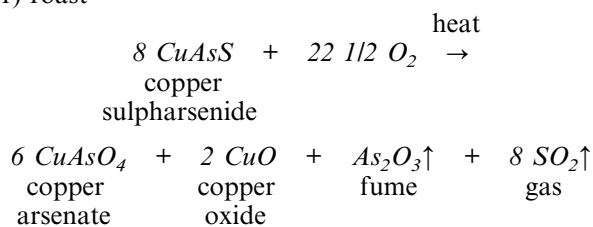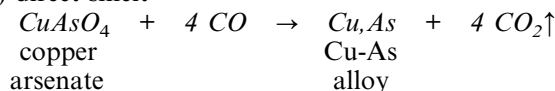
(1) roast

$$CuS \;+\; 1\,1/2\,O_2 \;\xrightarrow{heat}\; CuO \;+\; SO_2\uparrow$$
copper   oxygen   copper   gas
sulphide   oxide

(2) direct smelt

$$CuO \;+\; CO \;\rightarrow\; Cu \;+\; CO_2\uparrow$$
copper   copper
oxide   metal

If the ore is a sulpharsenide, containing both copper and arsenic, different reaction products result upon roasting.

(1) roast

$$8\,CuAsS \;+\; 22\,1/2\,O_2 \;\xrightarrow{heat}$$
copper
sulpharsenide

$$6\,CuAsO_4 \;+\; 2\,CuO \;+\; As_2O_3\uparrow \;+\; 8\,SO_2\uparrow$$
copper   copper   fume   gas
arsenate   oxide

(2) direct smelt

$$CuAsO_4 \;+\; 4\,CO \;\rightarrow\; Cu,As \;+\; 4\,CO_2\uparrow$$
copper   Cu-As
arsenate   alloy

Both copper and arsenic are oxidized during the preliminary roast to form a copper arsenate and arsenious trioxide (As_2O_3), a white fume or smoke.

In a single, direct smelting experiment (no. 3401), Lechtman dead roasted a rich enargite ore (Cu_3AsS_4), then smelted the oxide product in an experimental, Batán Grande-type furnace. The charge was a mixture of roasted ore and charcoal, in a 3:1 ratio, by
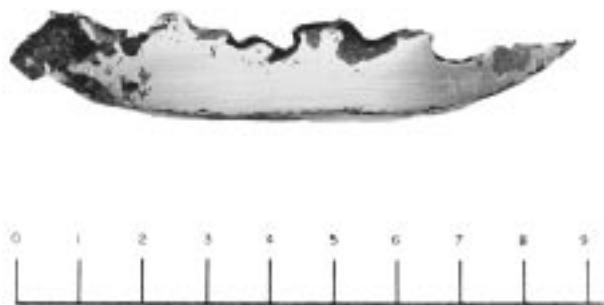
3401

Figure 1. Section through alloy ingot 3401: product of roasted enargite ore, direct smelted in furnace with charcoal. As polished.

Table 1. *Furnace direct smelting experiment (3401): chemical analyses of original ore, roasted ore, and alloy ingot*

	Cu	As	Sb (Weight%)	Fe	S
Original ore					
Mina Volare MIT 3327	41·6	15·6	1·11	3·90	32·00
Roasted ore MIT 3353	51·8	5·3	0·64	4·23	6·40
Product					
Alloy ingot MIT 3401	87·1	7·0	1·12	3·00	0·34

Elements were analysed by atomic absorption spectrometry (n.d., not detected; n.a., not analysed).

weight. The smelt produced a perfect ingot (Figure 1) containing 7·0 weight% As. Chemical analysis of the original enargite and of the roasted ore, presented in Table 1, provides a measure of the extent of arsenic and sulphur loss during roasting: 66% of the arsenic was lost as $As_2O_3\uparrow$; 80% of the sulphur escaped as $SO_2\uparrow$. Only trace amounts of sulphur remained in the smelted alloy ingot.
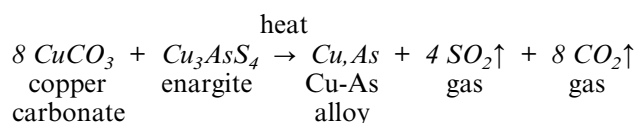
To date, there is no archaeological evidence to support the suggestion that early metalworkers produced arsenic bronze by roasting sulpharsenide ores, then direct smelting the oxide products of the roast. Nevertheless, a considerable body of literature argues that the production of noxious As_2O_3 fumes resulting from the two-step smelting process must have posed serious, long-term health hazards to communities of smelters (see Charles, 1979, 1980; Lechtman, 1996). This literature sustains that the gradual replacement of arsenic bronze by tin bronze in the Near East, over a period of almost two millennia, was occasioned, in part, by the effects of liberating toxic arsenic fumes into local environments.
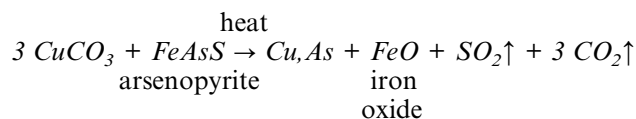
Cosmelting

Sulphur, present as sulphide in the metallic mineral portion of a primary ore, can reduce copper oxide ore to metallic copper in a cosmelting operation. Rostoker and his colleagues (Rostoker, Pigott & Dvorak, 1989) review the thermodynamic conditions under which the extraction of copper from its oxides can be accomplished with sulphur as the reducing agent. Charcoal need not fuel the smelt, since the generation of carbon monoxide is unnecessary. In cosmelting, oxide and sulphide ores are mixed and charged into furnace or crucible. At sufficiently high smelting temperatures, the sulphur extracts oxygen from the oxide ore, thereby reducing the ore, and is eliminated as sulphur dioxide. The following generalized equations present typical cosmelting reactions in which the sulphide mineral also contains arsenic. The product of the cosmelt is a copper–arsenic alloy.

Cosmelting copper oxide ores with copper or iron sulpharsenide ores

(1) Smelting with enargite

$$8\,CuCO_3 + Cu_3AsS_4 \xrightarrow{heat} Cu,As + 4\,SO_2\uparrow + 8\,CO_2\uparrow$$

copper enargite Cu-As gas gas
carbonate alloy

(2) Smelting with arsenopyrite

$$3\,CuCO_3 + FeAsS \xrightarrow{heat} Cu,As + FeO + SO_2\uparrow + 3\,CO_2\uparrow$$

arsenopyrite iron oxide

Sulphur is oxidized through its action as a reducing agent. It escapes as a gas, thus eliminating the need to preroast the sulphide ore. When the charge contains a sulpharsenide ore of copper or of iron, eliminating the roasting step dramatically reduces the opportunity for oxidation of arsenic to As_2O_3 fume.

Several other cosmelting products may accompany the metal or alloy, depending upon the concentrations of sulphur and iron in the charge. These include (1) matte: sulphides of copper or of copper and iron (e.g., CuS, Cu_2S, Cu_5FeS_4); (2) speiss: arsenides of copper and iron; (3) slag: when sufficient silica (SiO_2) is present in the rocky portion of the ore, it combines with iron oxide (FeO) to form slag, often of fayalite composition (Fe_2SiO_4). We discuss these by-products in our presentation of each cosmelting experiment.

The mixing of oxide and sulphide ores need not be deliberate. In most copper ore deposits, only the uppermost, fully oxidized zone is free of sulphide mineral. As miners deplete this zone, and as they approach the primary ore body, they frequently encounter ore that is partially weathered, containing mixtures of primary sulphides and oxide alteration products. Such ore constitutes a natural cosmelting

charge and would yield metallic copper or a copper–arsenic alloy upon smelting (Rostoker, Pigott & Dvorak, 1989). In the case of Batán Grande, in Peru, it appears that smelters did deliberately add arsenic-bearing ore to copper oxides, introducing a mixed charge to the furnace (Epstein, 1993; Merkel *et al.*, 1994).

Prior Experimental Work

Several studies report experiments in which copper ores were smelted to produce copper–arsenic alloys. Lorenzen (1965) smelted in crucibles; Tylecote (Tylecote, Ghaznavi & Boydell, 1977; Tylecote, 1980*a*) carried out furnace smelting. In both situations arsenic impurities present as natural constituents of the ores or of fluxes added to the charge contributed arsenic to the smelted copper. Rostoker & Dvorak (1991) directly reduced a deliberate mixture of malachite and synthetic copper arsenate with charcoal to produce an alloy containing 4·2 weight% As. In discussing the reduction smelting of arsenical copper oxides, Tylecote (1980*b*) calculated that, in ores containing less than 7 weight% As, most of the arsenic would be retained in the smelted metal. Tylecote suggested that copper–arsenic alloys of higher arsenic concentration, especially those that appear silver in colour, were produced through addition of high-arsenic minerals to the crucible. Pazuchin (1964: table 1) added orpiment (As_2S_3) directly to molten copper to produce copper–arsenic alloys containing from 3·6 to 4·9 weight% As. Between 77% and 88% of the arsenic in the mineral was transmitted to the alloy; speiss accounted for $\approx 5.5\%$ of the crucible product.

To challenge long-held assumptions that early metalworkers dead roasted sulphide ores, then direct smelted the oxidized product, several investigators set out to cosmelt oxide ores of copper with sulpharsenide ores, intending to produce copper–arsenic alloys. Pazuchin (1964) cosmelted copper oxide (CuO) or malachite [$Cu_2(OH)_2CO_3$] with orpiment, malachite with tennantite ($Cu_{12}As_4S_{13}$), and copper oxide with arsenopyrite (FeAsS). He achieved the best results with a charge of copper oxide and orpiment (5·7:1, by weight), heated in a graphite crucible to 1150°–1200°C. The smelted alloy contained 8·1 weight% As, 0·23% S; the recovery of arsenic to the alloy was 62%, and no speiss formed. The malachite-plus-tennantite charge (5:1) yielded an alloy containing 2·0 weight% As, 0·26% S; no speiss was reported. Pazuchin's experiments in cosmelting copper oxide with arsenopyrite had varied results. In all cases, the alloy product contained significant concentrations of iron. The experimental charge of 18 parts oxide: 1 part arsenopyrite resulted in an alloy containing 3·0 weight% As, 0·18% S, and 1·48% Fe; 97% of the arsenic was recovered from the ore. In the remaining arsenopyrite experiments, with oxide-to-sulphide ratios ranging

Table 2. Ore minerals cited in the text

Mineral	Chemical formula
Aragonite	$CaCO_3$
Arsenopyrite	FeAsS
Atacamite (hydrated form)	$Cu_7Cl_4(OH)_4 \cdot H_2O$
Azurite	$Cu_3(OH)_2(CO_3)_2$
Bismuthinite	Bi_2S_3
Brochantite	$Cu_4(SO_4)(OH)_6$
Chalcopyrite	$CuFeS_2$
Enargite	Cu_3AsS_4
Hematite	Fe_2O_3
Malachite	$Cu_2(OH)_2CO_3$
Olivenite	$Cu_2(AsO_4)OH$
Orpiment	As_2S_3
Paratacamite	$Cu_2Cl(OH)_3$
Pyrite	FeS_2
Quartz	α-SiO_2
Realgar	As_2S_2
Scorodite	$FeAsO_4 \cdot 2H_2O$
Siderite	$FeCO_3$
Tennantite	$Cu_{12}As_4S_{13}$
Tenorite	CuO

from 9:1 to 4·5:1, the smelted product consisted of a mixture of alloy and speiss, with arsenic concentration in the metallic portion reaching 8·6 weight%.

Rostoker & Dvorak (1991) carried out their co-smelting experiments in covered fireclay crucibles. The charge consisted of malachite, sodium carbonate, and crushed slag to which realgar (As_2S_2) or arsenopyrite was added. In one experiment, the oxide portion of the charge contained malachite and synthetic copper arsenate; chalcopyrite ($CuFeS_2$) was the sulphide component. Cosmelting with realgar produced copper–arsenic alloys with arsenic concentrations ranging from 2·9 to 9·9 weight%. As the ratio of charged oxide to sulpharsenide decreased, the alloy produced contained increasing amounts of matte or speiss distributed throughout the metal or floating above it. The single experiment reported for the cosmelting of malachite and arsenopyrite resulted in an alloy with low arsenic (0·9 weight%) but also low iron (0·2%).

Lechtman's (1985) cosmelting field experiments, reported here, differ from the others in several respects: (1) all the ores charged, except for arsenopyrite, were gathered on geological survey in Peru (Lechtman, 1976) and represent ore types that are likely to have been used by early metalworkers; (2) no synthetic compounds were included; (3) no fluxes or other materials were added to the smelting charge; (3) the experiments were carried out in furnaces built to approximate archaeologically-known smelting furnaces used in the Andean culture area to produce copper–arsenic alloys.

Table 2 lists the ore minerals used in the experiments reported here and in those carried out by other investigators, as well as minerals collected at Batán Grande excavation sites.

Cosmelting Experiment Design

The experiment site was located in Ashdown Forest, England, near the town of Wych Cross, Sussex. Cosmelting experiments were carried out in furnaces and in crucibles. The charges for both consisted of ores comminuted to 0·7–0·8-cm pieces, mixed to provide three distinct proportions of oxide to sulpharsenide—2:1, 3:1, 4:1, by weight. No flux was added to the charge. The furnace operations required that some charcoal be fueled to the furnace during the smelt to maintain combustion and adequate heat. It was convenient to mix charcoal with the ore and to feed ore and fuel together continuously as a combined charge. We used commercial charcoal, screened to a 0·6–1·3-cm size, and added it to the ore in quantities ranging from 10 to 30% of the combined weight of the charge.

Furnaces

Several small, bowl furnaces were built to approximate the size and shape of furnaces used at Batán Grande, Peru to produce copper–arsenic alloys (Shimada, Epstein & Craig, 1982: figure 4). Figure 2(a) illustrates the design and dimensions of the Wych Cross furnaces. A clay embankment at the site provided material for the furnace walls, and ordinary building brick and roof tile served as both fill and extra support beneath the tuyere. All interior furnace walls were coated with a thin layer (≈0·8 cm) of refractory stoneware clay (rated at 1200°–1300°C); a final skim coat of patching sand (a mixture of local clay and washed silica sand) was applied to bring the thickness of the interior lining to about 1 cm.

Hollow iron pipe with a 1-inch (2·5 cm) inner diameter served as a single tuyere. We outfitted the distal end with a refractory clay tip with a 1-cm internal bore. The end of the refractory nozzle was positioned 8 cm above the furnace floor. The proximal end of the tuyere attached to an old vacuum cleaner that blew air into the furnace; the rate of air flow was regulated and monitored by flow metres. In a typical furnace smelt, air flow rates varied between about 200 and 240 l/min.

We measured the temperature inside the furnace with a chromel–alumel thermocouple protected within a quartz sheath. The thermocouple bead emerged just in front of the rear furnace wall, 2 cm above the floor.

To insulate a furnace from the damp ground and to ensure adequate heat retention within the furnace chamber, we placed each unit inside a 60 cm deep, circular pit and surrounded it with rammed fragments of fired clay. The top of the furnace was flush with the ground. Figure 2(b) indicates the layout. A drainage channel surrounding the pit further inhibited the passage of ground moisture to the furnace enclosure.
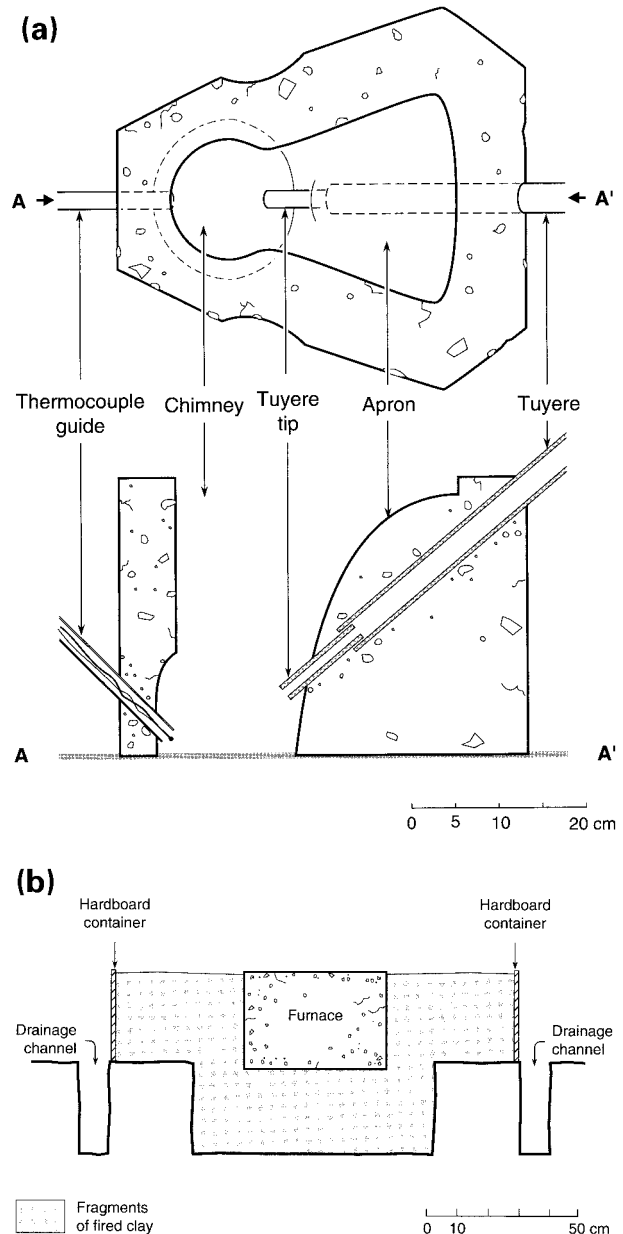

Figure 2. The experimental furnaces: (a) plan and section through a typical WC furnace; (b) sketch showing placement and insulation of a furnace in the ground.

The experimental furnaces incorporated the three main features that characterize the Andean model (see Figure 2(a)): (1) a small, bowl-like enclosure at the deepest level where the primary chemical and physical reactions take place; (2) a tall, narrow chimney at the rear of the furnace; (3) a steeply sloping "apron" at the front. Several aspects of the Wych Cross (WC) furnaces depart from the Batán Grande (BG) design. The overall pear- or keyhole-shape is somewhat more exaggerated in the BG furnaces. Their chimney opening tends to be less oval and narrower, with an overhang that may have reflected radiant heat back

into the furnace interior. The WC chimneys are somewhat taller than BG chimneys.

The apron in the WC furnaces slopes steeply towards the front of the furnace, rising to the full height of the front wall. In the excavated BG furnaces, the apron rises only to about half the furnace height, then opens and fans out onto a trough-like ditch. The excavators explain that during a smelt, large, thick ceramic sherds were placed above the apron opening, effectively closing the upper portion of the front wall (Shimada, Epstein & Craig, 1982). Many such slag-wet, vitrified sherds have been found at Batán Grande smelting sites. After a smelt, the sherds were discarded, and the furnace contents removed via the apron opening.

Finally, the WC furnaces were outfitted with a single tuyere that forced air deep into the bowl. At Batán Grande, blowpipes with clay nozzles (*toberas*) were used by groups of up to three persons, standing together at the front of a furnace, blowing air into the interior. The standard bore diameter of the BG nozzles is 0·8 cm, slightly smaller than the 1 cm used in the WC ceramic tips. Given the unvitrified appearance of the BG clay nozzles and on the basis of the slagging pattern exhibited by the large Batán Grande sherds, Epstein (1993) argues that the blowpipe nozzles never entered deep into a furnace but were inserted in the slightly open chinks between adjacent apron sherds.

In spite of these differences, the overall size and configuration of the Andean and experimental furnaces were close. In a typical experiment, the bowl and chimney were preheated with charcoal until the coals glowed orange. In experiment 3396, discussed below, the preheat took a full hour, at which time the thermocouple read 1064°C at the rear of the bowl. The mixed charge of ore (oxide+sulpharsenide) and charcoal was introduced as a slow, continuous pour onto the hot charcoal bed at the top of the chimney. As the charge descended the chimney, new ore was introduced. In experiment 3396, charging continued for 14 min. During a "soak" period that followed the last charge of ore, each furnace continued to be fed charcoal alone, to maintain a steady internal temperature until the air blast was discontinued. In experiment 3396, the soak lasted for 37 min, for a total smelt time of 51 min (see Figure 3). Experiment 3396 consumed 5·3 kg of charcoal during a preheat of 1 h and 4·2 kg during a 0·6 h soak.

By maintaining the flow of air at 200–240 l/min it was possible to maintain furnace temperature, registered by the thermocouple, below 1200°C, although the temperature closer to the tuyere must sometimes have been higher. We estimated that the maximum temperature the BG furnaces likely achieved, with a blowpipe-forced air regime, did not exceed 1200°C. This estimate has since been confirmed by experiment (Merkel & Shimada, 1988) and calculation (Rehder, 1994). Rehder calculated that a furnace temperature of 1200°C could be maintained steadily within a typical
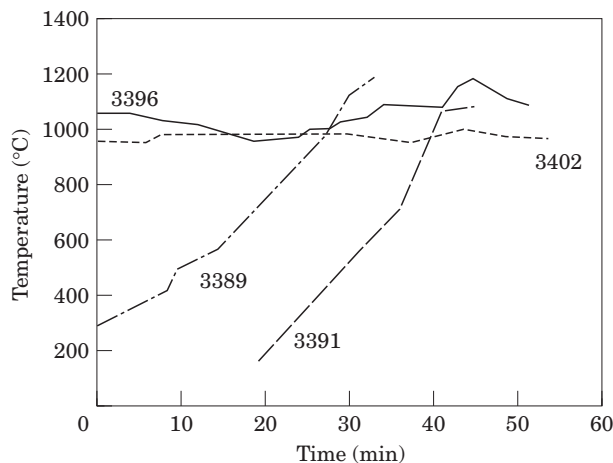

Figure 3. Time-temperature chart record for the four cosmelting experiments.

Batán Grande furnace by three individuals with blowpipes, blowing breath at an average flow rate of 0·22 m³/min (220 l/min) into the furnace bowl. Our vacuum cleaner supplied air, richer in oxygen than human breath, to the WG furnaces at the rate suggested by Rehder's calculations. The time versus temperature plot in Figure 3 for furnace cosmelt experiment 3396, a typical furnace run, shows how closely our air supply system approximated the prehistoric one presumed to have been used at Batán Grande (Merkel & Shimada, 1988).

When the WC furnaces were cold, we scooped and pulled the products out of the bowl through the chimney. Occasionally portions of the apron were removed to gain access to the furnace bottom. Our charges typically weighed about 1·9–2·2 kg. The volume of smelted material produced experimentally never exceeded 500 cc and was often about 300 cc. By comparison, Epstein (1993) reports that in the BG furnaces, the volume of the bowl below a line left by the surface of molten material (fused charge) is typically 1·25 l.

Crucibles

We used plumbago (a fired composite of graphite and fireclay) crucibles for the crucible cosmelting experiments. Filled with a comminuted, mixed-ore charge weighing 500 g, each crucible was heated in a cylindrical, natural draught furnace built with clay from the site. The furnace stood 0·55 m high, with an outer wall diameter of 0·6 m; the inner diameter of the central shaft measured 0·33 m. Coke served as fuel. The crucibles stood on a grate located 0·15 m above the hot coke bed.

Having preheated the furnace, we introduced the unlidded crucible and heated it slowly, by natural draught, for approximately 25–30 min. At a crucible temperature of about 700°C, we lidded the crucible and

engaged a blower to force air onto the burning coke bed. This raised the crucible temperature rapidly and ensured that the contents were fully molten at the time of pour. After about 5–7 min of forced air heating, the contents of most crucibles had reached 1050°–1190°C (see Figure 3). The molten material was poured into a hemispherical sand mould (1 part bentonite clay : 20 parts washed, fine grained builders' sand) and allowed to cool to ambient temperature.

During the smelts, we monitored the temperature inside the crucibles with a chromel–alumel thermocouple. In several experiments we observed some white smoke emanating from the crucible 12–15 min after the natural draught heating began, but this ceased abruptly and was not noted thereafter.

Raw materials

Oxide ores: copper chloride ores, primarily a hydrated form of atacamite [$Cu_7Cl_4(OH)_4 \cdot H_2O$] and paratacamite [$Cu_2Cl(OH)_3$], were the oxides smelted in the experiments. They come from two mines in the Acarí region of the Peruvian south coast. The igneous rocks hosting these secondary copper ores are associated with the coastal batholith (Vidal, 1985).

Mina Bella Unión: atacamite; brochantite [$Cu_4(SO_4)(OH)_6$]; azurite [$Cu_3(OH)_2(CO_3)_2$].

Mina Cobre Pampa: several copper chlorides, in addition to atacamite and paratacamite; aragonite ($CaCO_3$); siderite ($FeCO_3$); haematite (Fe_2O_3).

Arsenic-bearing sulphide ores: the sulpharsenide ores were enargite (Cu_3AsS_4) and arsenopyrite (FeAsS). The enargite ores are from two mines in the high *puna* of northern Peru. The arsenopyrite is from Gold Hill, Utah (U.S.A.) and was purchased from Ward's Natural Science Establishment, Inc.

Mina Volare: Sinchao region, limestone host rock; in addition to enargite, the ore contains minor amounts of pyrite (FeS_2) and quartz (α-SiO_2).

Quiruvilca: tertiary volcanic rock environment; enargite ore is extremely pure.

Gold Hill: dressed, reagent grade (95%) arsenopyrite; the remaining 5% includes quartz and bismuthinite (Bi_2S_3).

Table 3 presents the results of atomic absorption and neutron activation analyses of the ores. The main difference in composition between the oxide ores from the two source mines is their iron content. The two enargite ores are chemically similar. Iron, arsenic, and sulphur are the major elements in the arsenopyrite ore, which contains a negligible level of copper and a high concentration of bismuth.

Charcoal and crucible material: Table 4 gives the results of neutron activation analyses of the charcoal fuel, ashed charcoal, and of the plumbago crucibles.

Extractive Metallurgy

Eight crucible cosmelting experiments were carried out with charges whose oxide: sulpharsenide ore mineral content ranged from 1:1 to 4:1, by weight. A 3:1 oxide:sulpharsenide charge ratio was maintained in a series of 12 furnace cosmelting experiments. The only unsuccessful run was a crucible cosmelt with a 1:1 ore ratio charge.

We focus here on two sets of experiments that facilitate comparison between crucible and furnace cosmelting. In each set identical or highly similar charges of ore and fuel were smelted in a crucible and in a furnace. A 3:1 ratio of oxide: sulpharsenide ore was maintained throughout. Figure 4 indicates the main features of each experiment and the relationships between the two sets. The total weight of the charge and the principal elements present in each charge are presented in Table 5. We analysed the bulk composition of the smelting products by atomic absorption spectrometry or neutron activation (Table 6). Identification and composition of individual phases within the products were obtained by electron microanalysis and X-ray diffraction; point counting determined the phase volume fractions (Tables 7–10).

Set 1: crucible cosmelting with oxide and enargite (MIT 3389)

The smelt produced a perfect plano-convex metal ingot, topped by a thin, dense, dark grey crust and surrounded by a thick layer of granular material (Figure 5). The granular material had formed in the crucible. The underside of the ingot is full of large, spherical pores, but the top is perfectly smooth.

Table 6 shows that the ingot is a copper–9·7 weight% As alloy, which accounts for its pale pink colour. Sulphur concentration is low: 0·39 weight%. The ingot microstructure (Figure 6) is characterized by large, primary white dendrites of α-(Cu,As) surrounded by blue, interdendritic material of the γ-phase Cu_3As. Distributed homogeneously throughout the matrix are globules of darker blue matte material, whose composition approximates Cu_2S. Bismuth–copper inclusions, too small to see in Figure 6, are aligned along the interfaces between the primary and interdendritic phases. At the bottom of the ingot there is a tendency for the primary phase to coat the surface, presumably an effect of inverse segregation.

The crust (Figure 7) consists of large grey dendrites of matte (a mixture of Cu_8S_5 and Cu_2S) in a groundmass of interdendritic material composed of CuCl (nantokite) and [$Ca_3(SO_3)_2SO_4$] (calcium sulphite sulphate) (see Table 6 & Table 7). The bulk of the granular material is a mixture of quartz grains (α-SiO_2) and tiny matte dendrites (Cu_8S_5, Cu_9S_5, and Cu_9S_8) within a groundmass of CuCl (nantokite) (see Table 6 & Table 7). Table 7 indicates that the volume fraction of matte is the same in the crust and the granular material. The difference in the physical consistency of these two products results primarily from the abundance of quartz grains that make up the bulk of the granular material.

Table 3. Chemical analyses of ores used in experiments

	Cu	As	Sb (weight%)	Fe	S	Ag	Ba	Bi	Co	Mo (ppm)	Ni	Pb	Sn	Sr	Zn	SiO$_2$	Al$_2$O$_3$	CaO	K$_2$O (weight%)	MgO	MnO	TiO$_2$	P$_2$O$_5$	Cl
Oxide ores																								
Atacamite & Paratacamite Mina Cobre Pampa MIT 3321*	30·9	<0·005	<0·001	1·95	n.d.	15	2161	3042	3	5953	n.d.	25	2	106	n.d.	6·29	0·71	2·22	0·67	n.d.	n.d.	0·03	0·04	14·0
Atacamite & Paratacamite Mina Cobre Pampa MIT 3321†	10·0	<0·005	<0·001	1·38	n.d.	2	2605	6	4	1284	n.d.	39	10	163	22	9·69	3·26	13·77	1·61	0·02	0·02	0·06	0·04	7·36
Atacamite Mina Bella Unión MIT 3324	18·1	0·01	<0·001	16·84	n.d.	1	64	5	856	45	320	96	5	61	71	17·93	2·48	2·86	0·54	0·83	0·22	0·16	2·23	5·24
Sulphide ores																								
Enargite Quiruvilca MIT 3315	43·3	16·0	1·92	3·21	33·0	510	n.d.	250	n.d.	n.d.	n.d.	1500	2300	n.a.	3100	n.d.	<0·05	n.d.	n.a.	<0·005	0·009	n.a.	n.a.	n.a.
Enargite Mina Volare MIT 3317	42·4	15·7	1·18	4·01	32·7	120	400	n.d.	n.d.	n.a.	n.d.	300	300	n.d.	170	1·07	0·27	n.d.	n.a.	n.d.	n.d.	n.a.	n.a.	n.a.
Arsenopyrite Gold Hill MIT 3333	0·023	35·8	1·15	27·0	15·4	50	n.a.	28000	110	n.a.	70	2300	n.d.	n.d.	1200	14·97	0·10	n.d.	n.a.	0·007	0·02	n.a.	n.a.	n.a.
Arsenopyrite Gold Hill MIT 3335	0·015	35·0	1·42	26·7	16·4	31	n.a.	40100	110	n.a.	70	1500	n.d.	n.d.	2000	14·33	0·05	n.d.	n.a.	<0·004	0·02	n.a.	n.a.	n.a.

Elements were analysed by atomic absorption spectrometry (n.d., not detected; n.a., not analysed). *Portion of ore used in cosmelting experiments 3389 and 3391; †portion of ore used in cosmelting experiment 3402.

Table 4. Chemical analyses of charcoal fuel and plumbago crucibles used in experiments

| | SiO$_2$ | Al$_2$O$_3$ | CaO | Na$_2$O | K$_2$O | MgO | MnO | TiO$_2$ | P$_2$O$_5$ | Ag | As | Ba | Bi | Co | Cu | Fe | Mo | Ni | Pb | S | Sb | Sn | Sr | Zn |
				(weight%)												(ppm)								
Charcoal fuel/ash																								
Wood charcoal	0·71	0·14	1·49	0·02	0·77	0·18	0·04	<0·01	0·07	<0·4	<2	39	<5	2	5	909	<5	5	<5	n.a.	<0·2	n.a.	59	8
Ashed charcoal	4·24	1·21	59·88	0·65	22·45	7·76	0·66	0·06	2·27	<0·4	3	619	<5	9	4	3707	<5	2	<5	n.a.	<0·2	n.a.	1679	9
Crucible material																								
Plumbago crucible	38·71	16·48	0·29	0·31	0·69	0·19	0·04	0·66	0·03	<0·4	5	166	<5	10	40	31405	<5	70	<5	n.a.	0·9	n.a.	63	5

Elements were analysed by neutron activation (n.a., not analysed). Charcoal was ashed at 1000°C.
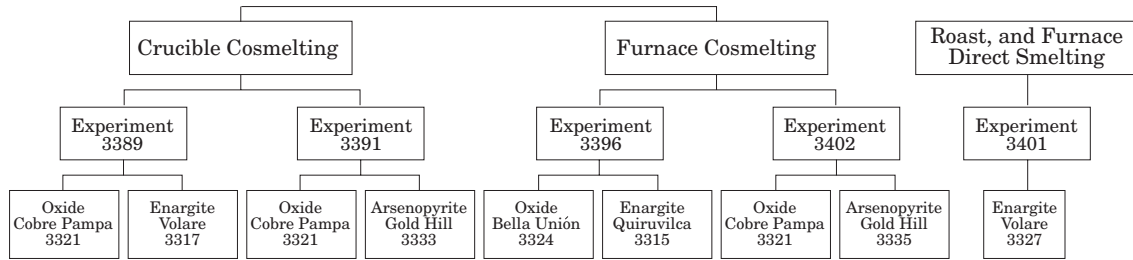
Figure 4. Flowchart indicating the number of each experiment, the raw materials used in each, and the relationships between experiment Sets 1 and 2.

Table 5. *Principal elements present in the crucible/furnace charge in each smelting experiment*

	Total charge (g)	Cu	As	Sb	Fe	S	Bi	SiO$_2$ (weight%)	Al$_2$O$_3$	CaO	K$_2$O	MgO	P$_2$O$_5$
Crucible cosmelting experiments													
MIT 3389													
Oxide+enargite 3:1 by weight	*500·0*	33·78	3·92	0·30	2·46	8·18	0·23	4·99	0·60	1·66	0·50	n.d.	0·03
MIT 3391													
Oxide+arsenopyrite 3:1 by weight	*500·0*	23·18	8·95	0·29	8·21	3·85	0·93	8·46	0·56	1·66	0·50	n.d.	0·03
Furnace cosmelting experiments													
MIT 3396													
Oxide+enargite+fuel ash 3:1 by weight	*2014·9*	24·30	3·99	0·48	13·38	8·22	<0·01	13·41	1·86	2·37	0·49	0·65	1·68
MIT 3402													
Oxide+arsenopyrite+fuel ash 3:1 by weight	*1353·3*	7·39	8·61	0·35	7·59	4·04	0·99	10·75	2·44	11·07	1·52	0·13	0·06

Set 1: furnace cosmelting with oxide and enargite (MIT 3396)

The furnace product formed as a cake with three completely separated layers (Figure 8(a), (b)): a plano-convex metallic ingot at the bottom; a uniform (0·59-cm thick) and flat layer of light-grey, crystalline matte in the middle; and a thick layer of glassy green slag at the top. The matte and slag layers cleave neatly at their interface (see Figure 8(b)). Near the interface, the slag is crystalline and light grey-green; otherwise it is glassy and dark green (Figure 8(a)). Molten metal accumulated and solidified in a small depression scooped out of the furnace bottom, at its centre. The matte layer formed above and around the edges of the ingot (see Figure 8(b) & Figure 9). The surfaces of both the metal and the matte that solidified in direct contact with the furnace bottom exhibit many large, round pores (Figure 9). During solidification of the matte, tiny copper metal filaments grew into and filled matte pores (Figure 9). Copper metal also formed as a distinct solid band (0·015-cm thick) at the interface between metal and matte (Figure 10 & Figure 11) and filled fissures within the matte. The composition of the copper filaments and band were determined by electron microanalysis: 99·78 weight% Cu, ≤ 0·01% As, 0·03% Sb, 0·04% Fe, 0·07% S.

From Table 6 we see that the metal ingot is a Cu-7·1 weight% As-4·5% Fe alloy, containing only 0·76% S. The iron occurs in matte and speiss inclusions in the metal (Table 8). The metallic microstructure exhibits primary, white dendrites of α-(Cu,As) surrounded by interdendritic light-blue material of the compound Cu$_6$AsSb (Figure 12). Bismuth–copper inclusions (≤3 μm in diameter) are aligned along the interfaces between the primary and interdendritic material. Dispersed throughout the metal are large matte dendrites of dark grey-blue colour and of bornite (Cu$_5$FeS$_4$) composition, and copper–iron arsenides present as long, narrow laths or as irregular-shaped areas of light grey colour (Figure 13(a), (b), (c)). The arsenides belong to the group of speisses. In the irregular-shaped speiss phase, there are areas of a mottled structure in which two phases can be distinguished: an additional copper–iron arsenide phase and tiny matte inclusions. The combined speiss and matte components of the ingot comprise approximately 19·8vol% of the metal (see Table 8).

The matte is composed of several sulphides of various shades of blue. The lighter blue material, of bornite composition, has an internal feathery structure (Figure 14). Within this structure the matte composition has shifted towards a higher copper content.

Table 6. Chemical analyses of major products of crucible and furnace cosmelting experiments

	Cu	As	Sb	Fe	S	Ag	Ba	Bi	Co	Mo	Ni	Pb	Sn	Sr	Zn	SiO$_2$	Al$_2$O$_3$	CaO	MgO	MnO	TiO$_2$	P$_2$O$_5$
	(weight%)					(ppm)										(weight%)						
Crucible cosmelting experiments																						
MIT 3389																						
Oxide+enargite, 3:1 by weight																						
Products:																						
Alloy	87·6	9·70	0·69	0·037	0·39	230	n.d.	2700	n.d.	200	n.d.	n.d.	<500	n.a.	<50	n.d	n.d.	n.d.	n.d.	n.d.	n.a.	n.a.
Crust	57·4†	0·13	0·017	0·685	3·94	173	4026	62	6	24000	5	243	n.a.	95	168	2·62	0·12	0·54	<0·01	0·01	0·01	0·02
Granular material	33·1†	0·10	0·017	0·182	2·16	95	1553	<5	3	9500	4	113	n.a.	23	117	47·57	0·44	0·06	<0·01	<0·01	0·06	0·02
MIT 3391																						
Oxide+arsenopyrite, 3:1 by weight																						
Products:																						
Alloy	69·5	26·00	0·41	0·031	1·50	130	n.d.	10500	n.d.	<200	50	n.d.	n.d.	n.a.	n.d.	<0·1	n.d.	0·03	<0·005	<0·002	n.a.	n.a.
Bulk material	13·9	8·95	0·33	23·29	1·70	2	1868	2139	32	8599	29	423	4	135	686	24·21	2·19	2·87	n.d.	0·02	0·07	0·03
Furnace cosmelting experiments																						
MIT 3396																						
Oxide+enargite, 3:1 by weight																						
Products:																						
Alloy	82·5	7·10	2·44	4·5	0·76	660	n.d.	n.a.	2500	n.a.	700	800	2000	n.d.	860	n.d.	n.d.	n.d.	<0·005	n.d.	n.a.	n.a.
Matte	58·41	0·62	0·15	6·1	15·4	210	3	<5	1380	12	152	287	n.a.	n.d.	1087	0·13	0·03	0·03	0·03	0·05	n.d.	n.d.
Slag	9·2*	<0·01	0·003	12·9	0·14	2	486	<5	128	6	160	161	n.a.	530	281	42·71	7·02	21·02	3·64	0·67	0·32	2·34
MIT 3402																						
Oxide+arsenopyrite, 3:1 by weight																						
Product:																						
Bulk of cake	13·64	0·70	0·04	6·63	3·44	n.d.	157	8	15	1180	120	33	n.a.	290	22	19·80	2·51	46·26	1·00	0·07	0·12	0·51

Elements were analysed by atomic absorption spectrometry or neutron activation (n.d., not detected; n.a., not analysed). *Cu values calculated by difference; †Cu estimated by difference as a part of nantokite (CuCl).

Table 7. *Microprobe analysis of the products of crucible cosmelting experiment 3389: atacamite and paratacamite (3321)+enargite (3317), 3:1 by weight*

	Vol. fraction (%)	Cu	As	Sb (weight%)	Fe	Bi	S
Alloy ingot							
Primary phase: α-(Cu,As)	66·5	96·12	4·99	0·19	0·01	0·06	0·01
Interdendritic phase: γ-Cu$_3$As	28·8	71·72	27·85	1·36	<0·01	0·27	0·27
Metallic inclusions*: (Bi,Cu)	<0·1	7·50	n.d.	0·10	<0·01	92·28	<0·01
Matte inclusions: ~ Cu$_2$S	4·6	n.a.	n.a.	n.a.	n.a.	n.a.	n.a.
Crust							
Matte†: Cu$_8$S$_5$, Cu$_2$S	30·1	77·58	0·20	0·02	0·04	n.d.	23·92
Other phases†: CuCl, Ca$_3$(SO$_3$)$_2$SO$_4$	60·8	n.a.	n.a.	n.a.	n.a.	n.a.	n.a.
Granular material							
Matte†: Cu$_8$S$_5$, Cu$_9$S$_5$, Cu$_9$S$_8$	3·0	n.a.	n.a.	n.a.	n.a.	n.a.	n.a.
Other phases†: CuCl	50·5	n.a.	n.a.	n.a.	n.a.	n.a.	n.a.
Other phases†: SiO$_2$	40·1	n.a.	n.a.	n.a.	n.a.	n.a.	n.a.

Chemical determinations were carried out by X-ray microanalysis with an electron microbeam probe (wavelength dispersive). *Normalized analyses; †components determined by X-ray diffraction; n.d., not detected; n.a., not analysed.

Table 8. *Microprobe analysis of the products of furnace cosmelting experiment 3396: atacamite (3324)+enargite (3315), 3:1 by weight*

	Vol. fraction (%)	Cu	As	Sb (weight%)	Fe	Bi	S
Alloy ingot							
Primary phase: α-(Cu,As)	74·5	93·76	1·43	1·26	1·55	0·04	0·03
Interdendritic phase: Cu$_6$AsSb*	5·1	64·40	15·06	21·33	<0·01	0·07	0·04
Laths: Speiss (Cu–Fe arsenide)	3·8	24·92	38·03	0·21	35·05	0·03	0·12
Irregular shaped phase: Speiss (Cu–Fe arsenide)	5·8	19·88	38·58	0·21	40·07	0·06	0·09
Mottled phase: Speiss (Cu–Fe arsenide)	2·6	6·24	27·50	0·33	56·11	n.d.	0·16
Metallic inclusions: (Bi,Cu)†	<0·1	53·43	0·89	0·32	0·4	44·53	<0·01
Matte inclusions: ~ Cu$_5$FeS$_4$	7·6	n.a.	n.a.	n.a.	n.a.	n.a.	n.a.
Matte							
Matte‡†: Cu$_5$FeS$_4$, Cu$_{1.9}$S	95·1	63·56	0·25	0·01	10·07	n.d.	26·07
Eutectic†: Fe oxide	~1·2	2·69	0·01	0·01	67·34	<0·01	0·70
Eutectic, inclusions†: Speiss (Cu–Fe arsenide)	~1·2	4·23	6·99	0·18	84·31	0·055	0·18
Metallic globules§	2·5	n.a.	n.a.	n.a.	n.a.	n.a.	n.a.
Slag							
Crystalline material‡: Fe$_2$SiO$_4$, Fe$_3$O$_4$	n.a.	n.a.	n.a.	n.a.	n.a.	n.a.	n.a.
Amorphous material‡	n.a.	n.a.	n.a.	n.a.	n.a.	n.a.	n.a.

Chemical determinations were carried out by X-ray microanalysis with an electron microbeam probe (wavelength dispersive). *Schubert *et al.* (1957) identified this same compound by powder diffraction and specified it as Cu$_{72.4}$As$_{12.8}$Sb$_{14.8}$. This composition recalculated to its atomic weight fractions yields a composition almost identical with that reported here. †Normalized analyses; ‡components determined by X-ray diffraction; §because of the concentric, multicompositional structure of the globular inclusions, no analysis is presented here. n.d., not detected; n.a., not analysed.

The matte is cracked, and pure copper has grown into the cracks (Figure 14). Metallic globules of light blue material, often with a concentric, multi-phase structure, are dispersed through the matte. The matte also contains regions of eutectic microconstitutent, made up of a black iron oxide phase (Fe$_3$O$_4$) accompanied by small grey speiss inclusions (see Figure 15).

The slag is largely amorphous except for a semi-crystalline layer (3·98-mm thick) near the matte that contains fayalite (Fe$_2$SiO$_4$) laths. There is a clear division between amorphous and crystalline portions. Tiny, spherical inclusions of metallic or semi-metallic material occur sporadically. Chemical analyses of the matte and slag are presented in Table 6; phase identifications and compositions in the matte appear in Table 8.

Set 1: comparison of crucible and furnace cosmelted products, using enargite

The smelting products are distinct in their physical makeup. The furnace product underwent gravity-separation of three components: metal, matte, slag. The crucible product formed no slag; the matte produced remained embedded in a matrix of chlorides,

Table 9. Microprobe analysis of the products of crucible cosmelting experiment 3391: atacamite and paratacamite (3321)+arsenopyrite (3333), 3:1 by weight

	Vol. fraction (%)	Cu	As	Sb (weight%)	Fe	Bi	S
Alloy ingot							
Primary phase†*: γ-Cu₃As	86·1	69·43	29·22	0·31	<0·01	0·29	0·61
Polyhedral inclusions*: (Bi,Cu)	1·3	5·83	n.d.	0·13	<0·01	94·02	n.d.
Eutectic: ∼ Cu₂S	3	79·81	0·81	0·01	0·01	<0·01	20·30
Matte dendrites: ∼ Cu₂S	9·5	n.a.	n.a.	n.a.	n.a.	n.a.	n.a.
Dense, matte-rich material							
(a) Zone with fine dendrites:							
Fine dendrites+cubic crystals†: Fe₃O₄	28·2	0·85	0·55	0·07	65·16	0·25	0·07
Additional phases†: FeS, CuCl, SiO₂	63·3	n.a.	n.a.	n.a.	n.a.	n.a.	n.a.
(b) Zone with large dendrites‡:							
Dendrites: ∼ Cu₂S	n.a.	76·77	0·98	0·08	<0·01	n.d.	21·93
Groundmass: CuCl	n.a.	n.a.	n.a.	n.a.	n.a.	n.a.	n.a.
(c) Metallic material:							
Globules: ∼ γ-Cu₃As	n.a.	67·6	28·7	0·4	3·0	2·2	0·3

Chemical determinations were carried out by X-ray microanalysis with an electron microbeam probe (wavelength dispersive). *Normalized analyses; †components determined by X-ray diffraction; ‡material insufficient for point counting; n.d., not detected, n.a., not analysed.

Table 10. Microprobe analysis of the products of furnace cosmelting experiment 3402: atacamite and paratacamite (3321)+arsenopyrite (3335), 3:1 by weight

	Vol. fraction (%)	Cu	As	Sb (weight%)	Fe	Bi	S
Metal globules: Type I+Type II	20·5						
Metal globules Type I							
Primary phase: γ-Cu₃As	32·0	71·16	27·89	1·52	0·15	n.d.	0·23
Second phase (elongated): Speiss (Cu–Fe arsenide)	46·5	25·43	38·41	0·13	35·27	n.d.	0·17
Third phase (bridging): α-(Cu,As)	16·0	91·41	7·05	0·99	0·42	0·09	0·04
Metallic inclusions*: (Bi, Cu)	<0·1	3·48	n.d.	0·22	1·22	95·07	n.d.
Matte inclusions	5·5	n.a.	n.a.	n.a.	n.a.	n.a.	n.a.
Metal globules Type II							
Primary phase: α-(Cu,As)	74·4	94·46	6·56	0·40	0·63	0·01	0·03
Interdendritic phase: γ-Cu₃As	3·3	68·44	27·42	3·40	0·19	0·4	0·15
Grey laths: Speiss (Cu-Fe arsenide)	5·5	23·55	40·67	0·05	35·57	0·02	0·13
Grey phase: Speiss (Cu–Fe arsenide)	16·6	22·23	39·42	0·02	38·07	0·08	0·16
Metallic inclusions*: (Bi,Cu)	<0·1	7·70	n.d.	0·03	0·12	92·65	0·04
Matte inclusions	<0·1	n.a.	n.a.	n.a.	n.a.	n.a.	n.a.
Material surrounding metal globules	79·5						
Matte dendrites†: Cu₅FeS₄	n.a.	69·00	0·73	0·04	6·10	0·04	24·09
Other phases†: β-Ca₂SiO₄, Ca(Fe,Mg)SiO₄	n.a.	n.a.	n.a.	n.a.	n.a.	n.a.	n.a.

Chemical determinations were carried out by X-ray microanalysis with an electron microbeam probe (wavelength dispersive). *Normalized analyses; †components determined by X-ray diffraction; n.d., not detected, n.a., not analysed.

sulphates, and silica. It should be recalled that no fluxes (iron oxides or silica) were added to the charged materials. In all the experiments reported here, slags formed only when ores were self-fluxing, including fluxing through the addition of CaO, K₂O, and MgO from fuel ash, and when smelting temperatures were sustained long enough at sufficiently high temperature. Referring to Table 5, the crucible charge 3389 contained 4·99 weight% SiO₂ and 2·46% Fe; the furnace charge 3396 had 13·41 weight% SiO₂ and 13·38% Fe. In spite of the combined low weight fractions of silica and iron in the furnace ores, the contribution of calcium oxide from the fuel ash helped flux the

gangue sufficiently to produce a monticellite variety [Ca(Mg,Fe)(SiO₄)] of slag containing 21 weight% CaO (see Table 6) at temperatures held above 1000°C for the last 27 min of smelting; the furnace temperature reached a maximum of between 1100° and 1180°C for the final 10 min (see Figure 3). By contrast, the low concentration of these natural fluxes in the crucible ores precluded slag formation at the maximum temperatures achieved: 950°–1150°C for about 7 min. The temperature was also too low for sintering of the silica grains, leaving a granular and friable material mixed with matte to surround the crucible ingot. The crucible matte is a simple sulphide of

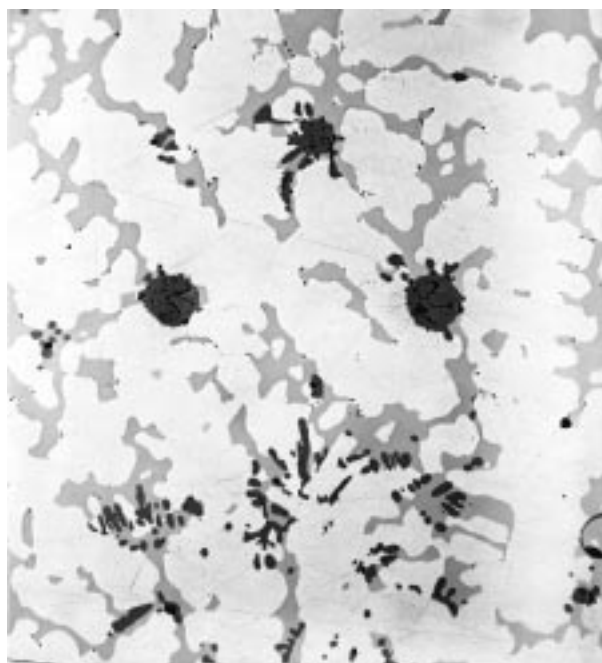Figure 5. Section through crucible cosmelting product 3389.

Figure 6. Microstructure of metal ingot 3389: large, primary dendrites of α-(Cu,As) alloy (white), with interdendritic Cu_3As material (light gray); Cu_2S matte present as dendrites and globules (black). Magnification 200. As polished.

Figure 7. Microstructure of crust 3389: dendrites of Cu_2S matte (white) in an interdendritic groundmass of nantokite and calcium sulfite sulphate. Magnification 100. As polished.

copper ($\approx Cu_2S$). The weight fraction of iron in the charge was too low for the formation of an iron-containing matte. Bornite (Cu_5FeS_4) matte formed in the furnace.

Although the chemical compositions of the ores are similar and the oxide: sulpharsenide ore ratio in the charges was identical, there are major differences between the two smelted ingots. The phase diagrams in Figure 16 facilitate comparisons between these alloys. The ingot produced in the crucible is 37% higher in arsenic than the furnace ingot. The crucible ingot contains trace amounts of iron and a minor amount of antimony, whereas in the furnace alloy iron is present as a major component, as is antimony. The crucible alloy 3389 is quite pure, containing only 4·6vol% of matte ($\approx Cu_2S$) inclusions. The furnace ingot 3396 contains a high-antimony interdendritic phase, two

speiss phases, and matte (Cu_5FeS_4) inclusions. Approximately 8% of the total arsenic in the furnace product is in the matte layer; 91% is present in the ingot.

During smelting, the higher overall loss of arsenic in the furnace as compared with the crucible resulted from differences in the manner of charging the ore and in isolating it from environmental oxygen. The crucible was charged once and remained without a lid until the final ≈ 5–7 min of the smelt. Shortly after smelting products began to form, however, a crust developed on the surface of the charge, slowing entry of gases into the crucible and escape of gas or fume from the reacting materials. The crust effectively inhibited surface oxidation of the charge with attendant formation of As_2O_3 fume. The furnace charge was added in batches throughout the course of the smelt. With each addition, some ore oxidized at the exposed, hot surface before there was time for the charge to drop into the furnace bowl. Even in spite of the burning charcoal mixed with the charge, the constant stream of air blowing into the bowl exposed the furnace mineral to higher oxygen levels than those experienced inside the plumbago crucible.

Iron partitioned among the metal, matte, and slag furnace products. Within the alloy, the high affinity of iron for arsenic resulted in the formation of Cu–Fe arsenides, or speiss. The furnace ingot contains approximately 12·2vol% of speiss, almost all the speiss produced in the smelt. These reactions, favoured by the limited solubility of arsenides in mattes (Kleinheisterkamp, 1948), are discussed further below.
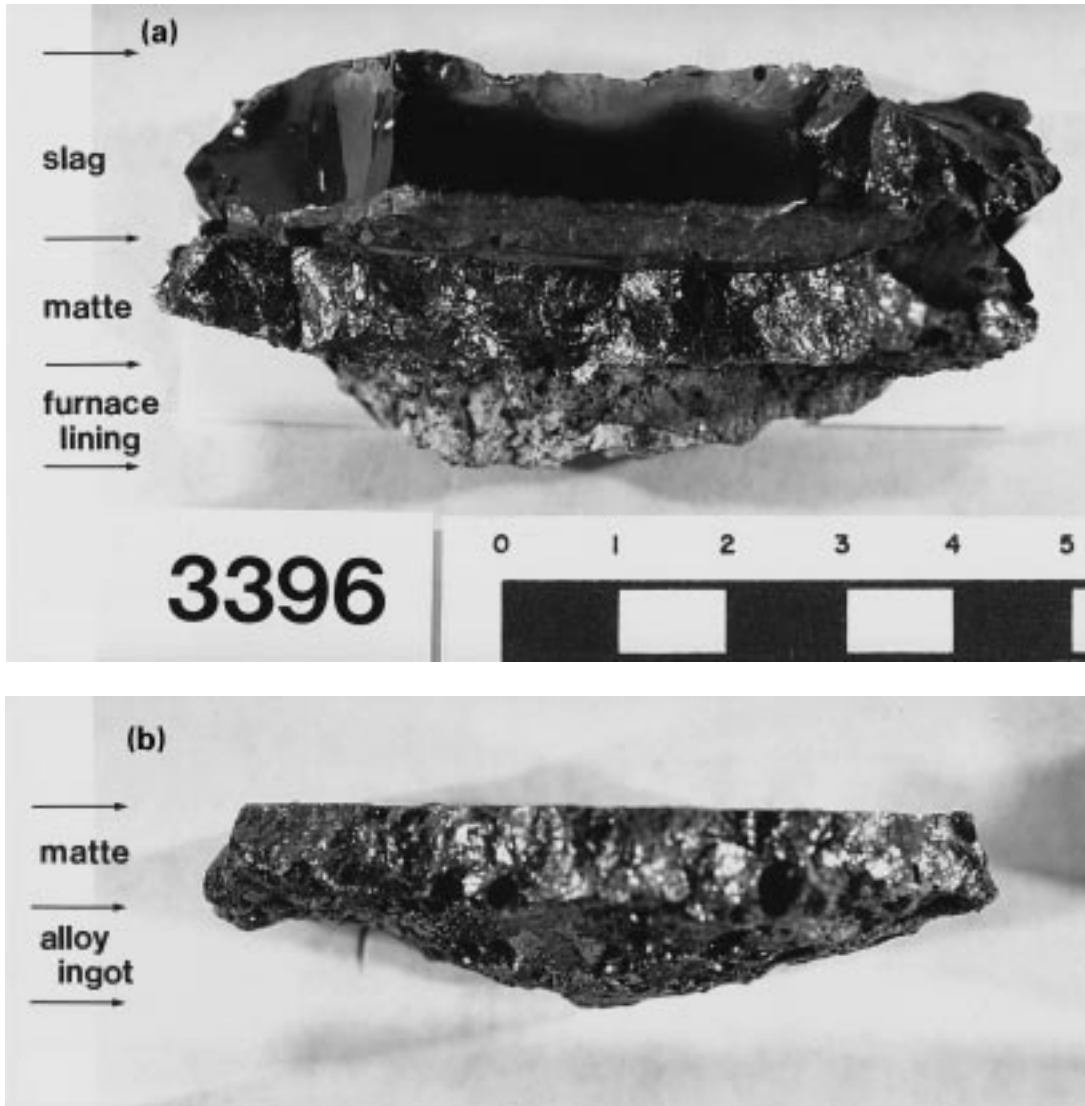
Figure 8. Section through furnace cosmelting product 3396, showing distinct layers of slag, matte, and alloy: (a) slag, matte, and furnace lining; note the thin layer of crystalline slag at the interface of slag and matte; (b) matte and alloy ingot.

Set 2: crucible cosmelting with oxide and arsenopyrite (MIT 3391)

The smelted product comprises two types of material (Figure 17): a metal ingot that formed at the bottom of the mould, and a dark and dense, matte-like material located above the metallic portion. The ingot, a Cu–As alloy containing 26·0 weight% As and 1·5% S (see Table 6), is bright, almost steelwhite, and highly reflecting. Its iron content is low: 0·03 weight%. The metallic microstructure (Figure 18) is characterized by large but fine matte (Cu_2S) dendrites and a darker grey eutectic microconstituent of matte material (Cu_2S) in a pale grey groundmass of primary γ-phase Cu_3As. The matte material constitutes approximately 12·5vol% of the ingot (see Table 9). Under slightly crossed polars one can see distinct, large lamellae in this groundmass which exhibit a small compositional shift with respect to the matrix material. Bright white, highly reflecting polyhedral inclusions of copper–bismuth composition ($\leq 40\,\mu$m in diameter) occur at grain boundaries. The ingot exhibits fine cracks, indicative of the extreme brittleness of the material. Tables 6 and 9 present the results of chemical analyses, X-ray diffraction, and electron microanalyses of crucible ingot 3391.

Two zones can be distinguished in the dense material above the ingot (see Figure 17): zone A, the bulk of the material, is located inside a surface layer or rind; zone B is a green surface layer. Zone A (Figure 19(a)) is made up of a grey groundmass of nantokite (CuCl) filled with extremely fine magnetite (Fe_3O_4) dendrites. Some regions show only this fine dendritic structure; in others there are dense accumulations of lighter grey, cubic iron oxide crystals. Iron sulphide (FeS) and
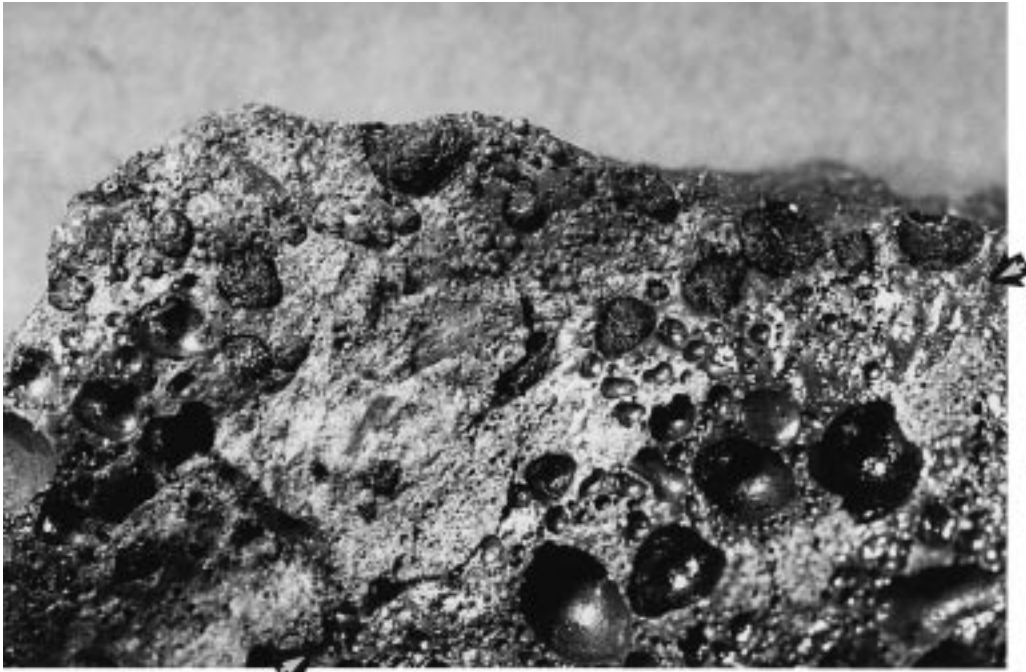
Figure 9. Detail of underside of furnace product 3396. Surface shown solidified in contact with the furnace bottom. Material above and left of arrows is matte; material below and right of arrows is alloy. Both materials are highly porous, but copper filaments grow only into pores located in the matte.

Figure 10. Section through matte layer and alloy ingot of furnace product 3396. Note thin layer of copper metal at the interface between matte and alloy. As polished.
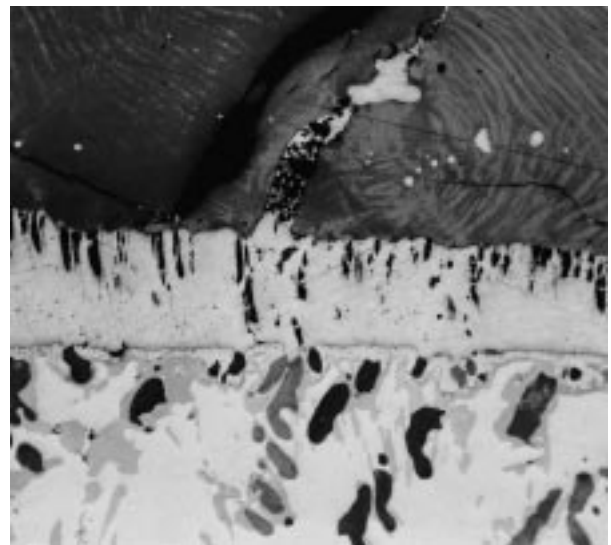
Figure 11. Detail of the matte/alloy interface shown in Figure 10: matte (top zone), copper (middle zone), and alloy (bottom zone). In addition to the broad band of copper that has formed between matte and alloy, some metallic copper has grown into a fissure in the matte. Magnification 100. As polished.

quartz (α-SiO_2) were detected by X-ray diffraction, and scanning electron microscopy identified some brown, block-like crystals as calcium silicate in character.

Zone B (Figure 19(b)), which corresponds to the green surface corrosion layer, is characterized by large, coarse, light grey dendrites of chalcocite (Cu_2S) in a groundmass of nantokite (CuCl). Interdendritic spaces are largely voids. Large, light grey globules of γ-phase Cu_3As also occur in this zone.

In spite of the presence of iron in the crucible charge (8·21 weight%; see Table 5), no bornite matte formed. Instead, most of the iron combined with oxygen to produce magnetite, which comprises 28·2 vol% of the dense, matte-rich material in zone A (see Table 9).
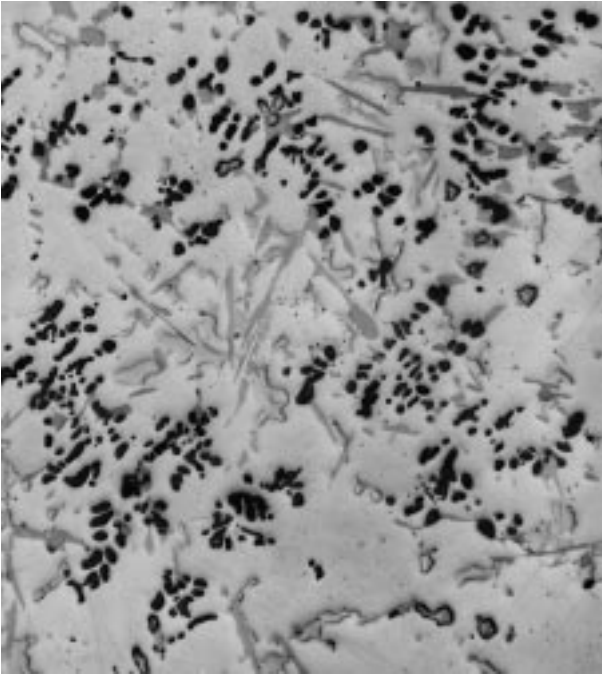
Figure 12. Microstructure of metal ingot 3396: primary dendrites of α-(Cu,As) alloy (white); long laths and irregularly shaped speiss phases (gray) and dendrites of Cu_5FeS_4 bornite-type matte (black) are interspersed throughout the metal. Magnification 50. As polished.

Bachmann (H.-G. Bachmann, pers. comm., 1998) has pointed out that, in spite of the presence of 23·29 weight% Fe and 24·21 weight% SiO_2 in the bulk material surrounding the ingot (see Table 6), no fayalite slag formed as a product of the smelt. During initial heating of the crucible charge, the arsenopyrite decomposed, its iron content oxidizing to magnetite. This spinel-type oxide is highly inert and stable, reacting only at temperatures above 1300°C. With iron in the charge stabilized as magnetite rather than as FeO, fayalite slags did not form.

Set 2: furnace cosmelting with oxide and arsenopyrite (MIT 3402)

The melt cooled inside the furnace to form a cake (Figure 20) consisting of a heterogeneous, porous mass of dense black material. The furnace cake is a mixture of bornite-type matte and various calcium silicates and sulphates: block-like β-Ca_2SiO_4, a $Ca(Fe,Mg)SiO_4$ (monticellite slag) phase, and cored calcium sulphate grains. Scattered throughout this matrix are tiny metallic or semimetallic prills of various compounds with Cu, As, Fe, and S (see Table 6 & 10). The concentration of sulphur in the entire cake is only 3·44 weight% (see Table 6), demonstrating how effective cosmelting was in eliminating sulphur from the furnace products. A roughly oval cap of dense, black material

formed at the top surface of the cake. Although the cap contains less metal in the form of disseminated prills, Figure 21 illustrates filaments of pure copper growing into pores in this surface layer. The cap consists of large grains of larnite (Ca_2SiO_4), a calcium silicate, and a calcium–alumino–chloride compound. Together with grains of bornite matte, these calcium-rich phases build a network within the cap.

The metallic portion of the cake never coalesced as an ingot. Metal prills, ranging in size from ≈1·5 to 0·02 mm in diameter, are distributed rather homogeneously throughout the groundmass, occasionally forming a coherent metallic network. Some prills are large enough to permit extraction by mechanical means. A few of the larger metallic prills were the subject of closer investigation. They exhibit two distinct structures. Type I prills (Figure 22) consist of a matrix of antimony-rich γ-phase Cu_3(As,Sb), with large, almost parallel laths of (As–Cu–Fe) speiss (Figure 23(a), (b), (c)), and an α-(Cu,As) phase that bridges the speiss laths. Matte dendrites (Figure 23(d)) accompany the speiss, and bismuth–copper inclusions are aligned along grain boundaries (Figure 23(a)). We consider Type I metal to represent an intermediate stage in alloy formation, given its high volume fraction of speiss (46·5%) and the presence of the α-phase (16·0vol%; see Table 10).

Type II prills (Figure 24), by contrast, contain a primary α-(Cu,As) phase that occupies 74·4vol% of the metal (see Table 10). Type II prills also have an interdendritic phase of antimony-rich γ-Cu_3(As,Sb) as well as grey laths and an irregular grey phase of (As–Cu–Fe) speiss. A few bornite-type matte inclusions accompany the speiss; copper–bismuth inclusions are aligned along grain boundaries. We present the results of X-ray diffraction and electron microanalyses of the phases present in prill Types I and II in Table 10.

Had the furnace operated at temperatures higher than 1000°C (see Figure 3), the Type II metal prills would likely have melted together to form an ingot at the bottom of the cake. We can calculate the approximate weight percent fractions of the elements present in such an ingot on the basis of the microanalyses and volume fractions of the phases reported in Table 10 for Type II prills. The ingot would have contained approximately 77·5 weight% Cu, 14·6% As, 8·8% Fe, 0·4% Sb, 0·02% Bi, 0·05% S.

Whereas furnace cosmelt 3402 was unsuccessful in producing a coherent copper–arsenic alloy ingot, it may represent most closely the characteristics of Batán Grande furnace operations as determined from archaeological and experimental evidence. The salient characteristics are: (1) a presumed mixed charge of copper oxide ore and either arsenopyrite or its weathered product, scorodite; (2) a smelt product consisting of viscous slag with entrapped copper and copper–arsenic alloy prills; (3) a furnace temperature that rarely exceeded 1100°C (Merkel & Shimada, 1988).
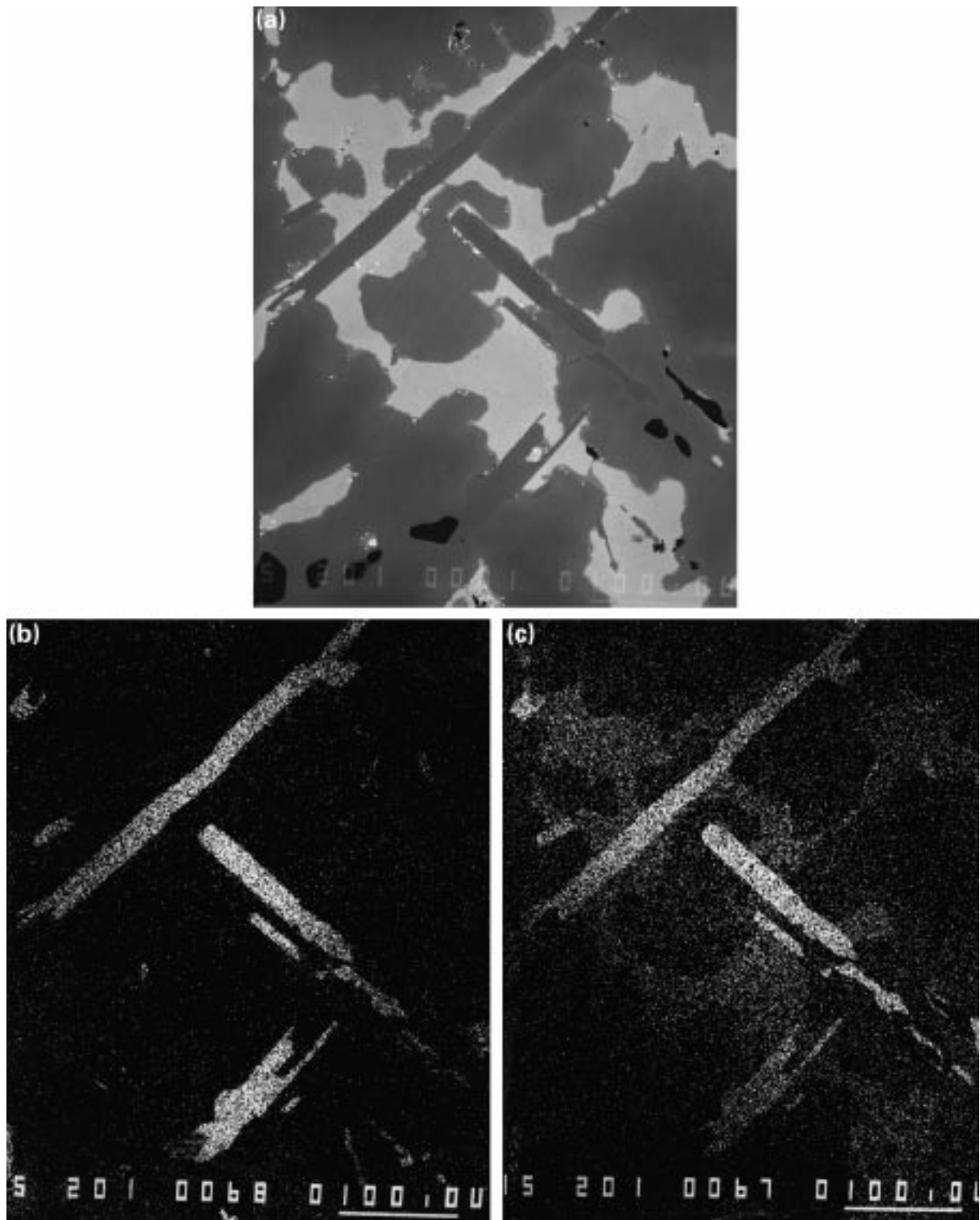
Figure 13. (a) Backscattered electron image of alloy ingot 3396. The primary α-(Cu,As) phase is grey; the interdendritic material (Cu$_6$AsSb) is white. The long, grey laths are copper-iron arsenides (speiss). (b) X-ray image for Fe K_α revealing the high iron content of the speiss phase shown in (a). (c) X-ray image for As L_α. The highest concentration of arsenic (38%) occurs in the speiss laths; the areas of interdendritic material, containing 15% arsenic, appear less dense on this X-ray image. Magnification 200 for each.
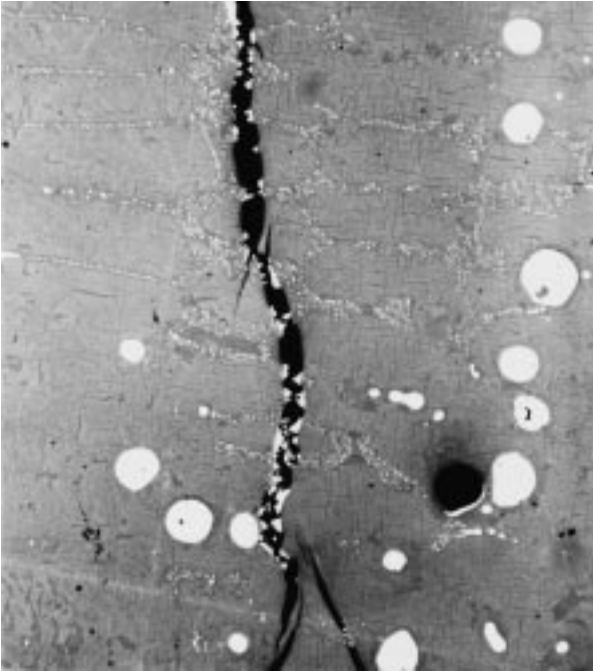
Figure 14. Microstructure of bornite-type matte 3396. The fine and highly oriented eutectic structure is indicated by small speiss inclusions (white) associated with an iron oxide eutectic microconstituent too small to be visible here, but shown (black) in Figure 15. Filaments of pure copper have grown into a crack in the matte. The large metallic globules (white) exhibit a concentric microstructure, not visible on this as-polished section: material at the centre is identical with the ingot alloy; material at the rim consists of speiss. Magnification 100. As polished.
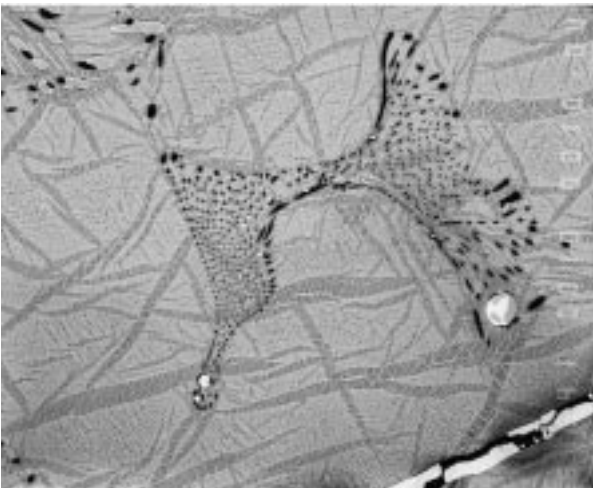
Figure 15. Backscattered electron image of matte 3396. Feathery structure of the bornite groundmass, with eutectic iron oxide microconstituent (black). Speiss inclusions (grey, upper left corner) have precipitated in association with the eutectic. Fissure (lower right corner), filled with metallic copper (white). Magnification 540. As polished.

Set 2: comparison of crucible and furnace cosmelted products, using arsenopyrite

Failure of the furnace cosmelting experiment (3402) to produce an ingot resulted from too low an operating temperature. The temperature versus time graph plotted in Figure 3 indicates that during the 55 min smelt the furnace reached 1000°C only twice, and briefly. Otherwise, the temperature varied around an average of approximately 980°C. Whereas this temperature was high enough to melt the metallic and semi-metallic prills and to allow some localized metallic networks to form, the furnace was never hot enough to melt the bulk of the matrix material. The prills were unable to migrate through the cake to the furnace floor. In the crucible experiment (3391), the charge attained temperatures between 900° and 1080°C for about 7 min, at the end of the smelt. This temperature range is well above the melting point (M.P.) of the Cu-26·0 weight% As alloy produced during the operation (M.P.=800°C; see Figure 25). The partially dendritic microstructures of the matrix material (see Figure 19(a), (b)) indicate that the bulk of the crucible cake was semi-molten or soft for a long enough period to allow the denser metallic portion to sink through it.

Since no coherent ingot was produced during the furnace smelt, we cannot make a detailed comparison between the Set 2 crucible and furnace alloy products. Nevertheless, both experiments yielded metal of high-arsenic content: 26·0 weight% in the crucible ingot, and approximately 6 weight% in the furnace Type II prills (see Table 10). The furnace would likely have yielded an ingot containing approximately 15 weight% As under slightly higher operating temperatures.

The phase diagrams in Figure 26 compare the types and abundances of phases that appear in the metallic products of the Set 2 cosmelting experiments. Like the diagrams drawn for the Set 1 experiments (see Figure 16), they show how clean the crucible alloy is in comparison with the furnace alloy (in Type II prills). The ingot contains only a small volume fraction of chalcocite matte; no speiss is present. The Type II furnace prills contain high volume fractions of speiss as well as bornite-type matte. Only the furnace matte exhibits pure copper filaments that have grown into some of the pores.

Discussion of the Experimental Results

Cosmelting oxide ores of copper with sulpharsenide ores, whether in a crucible or a bowl furnace, appears to be straightforward and yields coherent, clean Cu–As alloy ingots over a wide range of ore mixtures. Our crucible cosmelts were successful with charges whose oxide: sulpharsenide ore ratios varied from 2:1 to 4:1; a single experiment with a 1:1 charge was unsuccessful. All the furnace cosmelts were carried out with charges containing a 3:1 ratio of oxide to sulpharsenide ore. Except for a single furnace cosmelt with arsenopyrite (3402), the alloy ingots were easily mechanically separable from matte, slag, and granular by products. Almost all of the sulphur was eliminated from the metal won during cosmelting. Iron remained a major
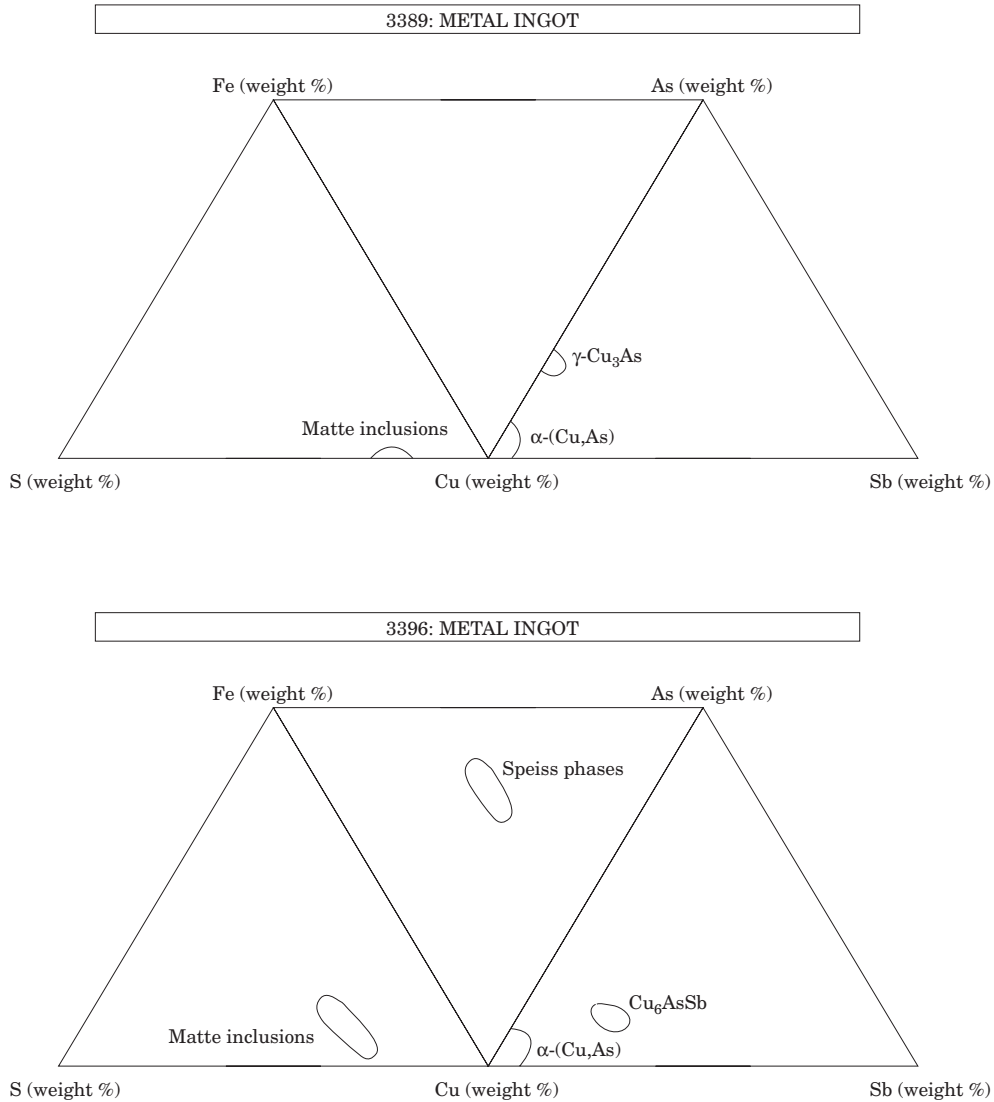
Figure 16. Combined ternary diagrams (As–Cu–Fe–S–Sb) showing the major components of metal ingot products 3389 and 3396. Outlined areas within the ternary triangles represent the spread in composition of inclusions and phases within each ingot. Mean compositions appear in Tables 6, 7 & 8. All compositions were determined by electron microanalysis.

contaminant ($4 \cdot 5 - \approx 8$ weight%) only in the furnace-produced alloys.

A major difference in the design and undoubtedly in the results of the crucible and furnace experiments arose from the location of the fuel and the consequent generation and availability of combustion gases during smelting. The furnace charges all contained charcoal, fed into the furnace from above. The burning charcoal produced some CO and CO_2 which, depending upon the partial pressure of oxygen within the enclosure, may have contributed to the reduction processes taking place. By contrast, the crucibles were heated from below; no charcoal was admixed with the charge of ore. Even during the initial heating stage, when the crucibles remained without a lid, it is unlikely that CO generated by the burning coke and surrounding the crucible would have been responsible for much ore

Figure 17. Section through crucible cosmelting product 3391. The highly reflecting alloy collected and solidified as an ingot at the bottom of the hemispherical mould.

Figure 18. Microstructure of ingot 3391: large grains of primary γ-Cu$_3$As alloy (pale grey) and Cu$_2$S matte dendrites (dark grey). Magnification 100. As polished.

reduction inside the vessel. As Bachmann has pointed out, "the furnace experiments are perhaps closer to archaeological reality and the crucible experiments nearer to unambiguous cosmelting with sulphur as the sole reducing agent" (H.-G. Bachmann, pers. comm., 1998). The operating distinction depends on whether or not, during the prehistoric and early periods we are considering, crucible smelting was carried out by heating crucibles from below, rather than by heaping charcoal on top of the charge and heating from above, approximating the furnace configuration.

Rostoker & Dvorak (1991) present the basic chemical reactions that occur during the cosmelting regimes they and we undertook. Here, Table 11 complies the principal components included in the charge and in the products of each smelting experiment. Table 5 records the principal elements present in the charged materials. The data in these two tables enabled us to calculate the recovery of key elements, such as arsenic, as they were extracted from the charge and passed into the products during smelting.

Recovery of arsenic and partitioning of iron

The arsenic content in the alloy ingots produced with arsenopyrite (3391: 26·0 weight% As; 3402: estimated 14·6 weight% As) is markedly higher than in those produced with enargite (3389: 9·7 weight% As; 3396: 7·1 weight% As). This is not surprising, as the arsenic content of the two sulpharsenide ores differs significantly (arsenopyrite: 36 weight% As; enargite $\approx$ 16

weight% As). The use of crucibles or furnaces for the cosmelting also influenced the recovery of arsenic: 28·4% of the charged arsenic was recovered in the crucible experiment (3389) with enargite; 23·2% of the charged arsenic was recovered in the furnace experiment (3396) with enargite; 92·6% of the charged arsenic was recovered in the crucible experiment (3391) with arsenopyrite. Under the operating conditions of this set of experiments, smelting in a crucible appears to be more efficient for arsenic retention, and the graphite content of the plumbago crucible probably further inhibited oxidation of arsenic to As$_2$O$_3$. The retention of arsenic in the furnace products would undoubtedly have been considerably higher had the charge been placed directly into the furnace bowl. Adding the charge intermittently from the furnace top gave the ore time partially to "roast" in air before dropping into the chimney column. In the case of the crucible smelts, recovery of arsenic to the ingot would certainly have been higher had the crucible been covered during the entire course of the smelt. Arsenic does not exceed 0·73 weight% in any of the semi- and non-metallic materials, whether produced in crucible or furnace, except in the arsenopyrite crucible experiment (3391) where it occurs in alloy prills in the crust (see Table 9).

We have already noted how clean the crucible ingots are with respect to their content of iron and iron-rich phases (3389: 0·037 weight% Fe; 3391: 0·031 weight% Fe). No copper–iron arsenides (speiss) and no iron-containing matte (bornite) inclusions appear in the crucible ingots. This is remarkable, especially in the case of crucible experiment 3391. By contrast, the furnace alloy products are characterized by high iron contents (3396: 4·5 weight% Fe; 3402: estimated 8·8 weight% Fe). The speiss phases and iron-containing matte inclusions are responsible for the iron impurities. In furnace cosmelt 3396, the atacamite ore (17 weight% Fe) was the chief supplier of iron to the charge. The high iron concentration in cosmelting product 3402 came from the arsenopyrite ore (27 weight% Fe). As crucible ingot 3391 demonstrates, however, the purity of the smelted alloy on the one hand, or the production and inclusion of iron-rich phases and matte on the other, cannot be explained solely by the nature of the raw materials. The smelting enclosure and environment—crucible or furnace—play an important role in the formation of particular phases.

The mattes

The crucible and furnace mattes differ in two respects. Chemically, the crucible mattes are of chalcocite (Cu$_2$S) composition; the furnace mattes are bornite (Cu$_5$FeS$_4$), containing up to 6 weight% Fe. This distinction in matte composition held regardless of whether the charge contained enargite or arsenopyrite, the latter contributing high concentrations of iron to the smelt. Physically, crucible mattes did not form
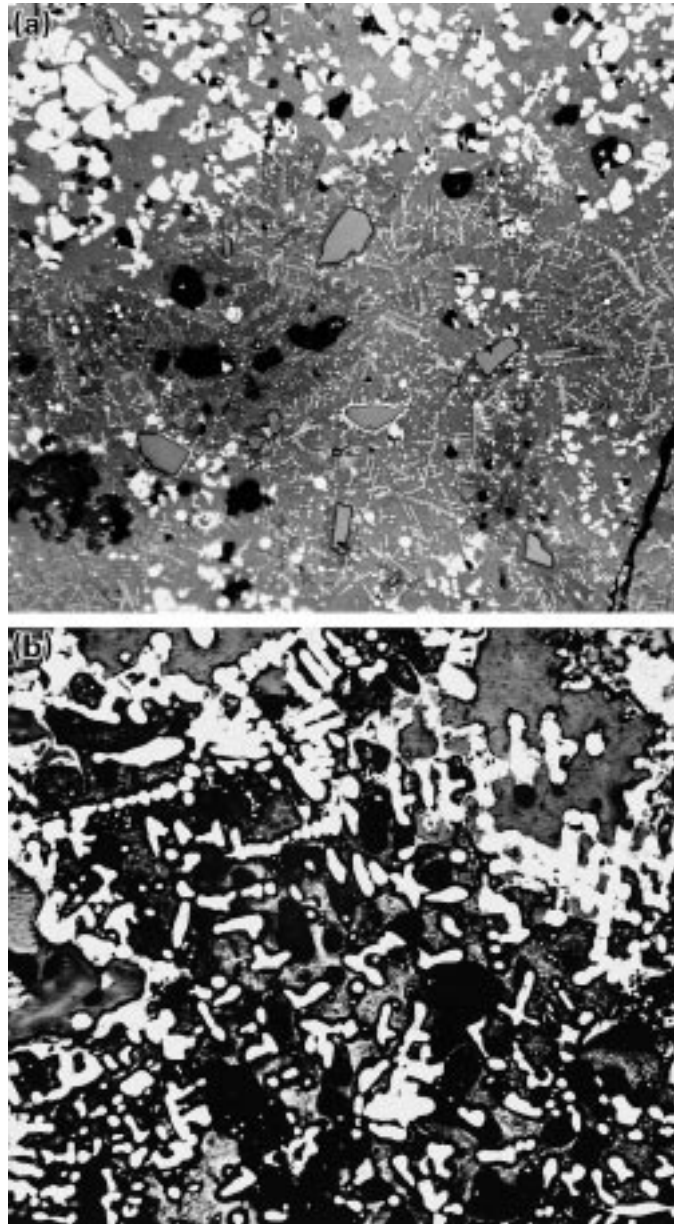
Figure 19. Microstructure of product 3391. (a) Zone A, bulk of material: fine dendrites and cubic crystals of iron oxide (white) in a groundmass of nantokite (CuCl); large, irregular grains (grey) are composed of calcium silicate. (b) Zone B, surface rind: large matte dendrites of Cu_2S (white) in a groundmass of nantokite. Magnification 200. As polished.

distinct, coherent layers or zones with respect to the ingots. Chalcocite matte tended to distribute homogeneously throughout the granular or crusty material surrounding the metal. In all the successful furnace cosmelting experiments, including several not reported here, the bornite mattes separated as perfect layers above the alloy ingots. We note that a slag will form, as it did in smelt 3396, when fluxing agents (such as CaO and K_2O) from the charcoal ash are present in sufficient abundance.

The composition of the matte and, in particular, of its iron-to-copper ratio, can vary significantly depend-ing on the amount of oxygen available to oxidize the iron out of the matte. Figure 27 shows matte compositions with a wide range in their iron-to-copper ratio, in equilibrium with magnetite and with silica-saturated iron–silica slag, and the corresponding oxygen solubilities. Clearly, the fact that the mattes in the crucible experiments contain little iron compared to the mattes in the furnace experiments is linked to the oxygen supply to the system under the conditions of the experiments. Preliminary calculations using the computer program Thermo-Calc (Sundman et al., 1985) indicate the importance not only of oxygen but
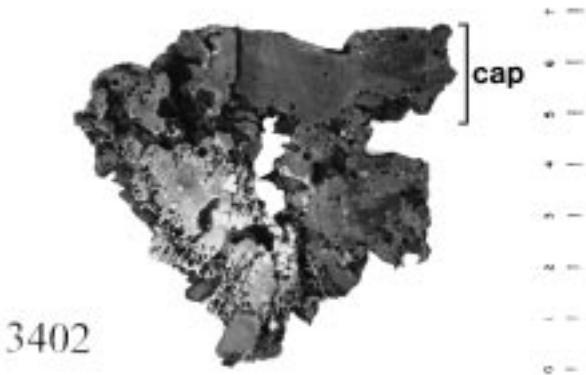
Figure 20. Section through furnace cosmelting product 3402, oriented as it solidified in the furnace. The metal has migrated towards the bottom of the cake as discrete prills and as a discontinuous network; no coherent ingot has formed. The metal is embedded in a silicate matrix containing bornite matte.
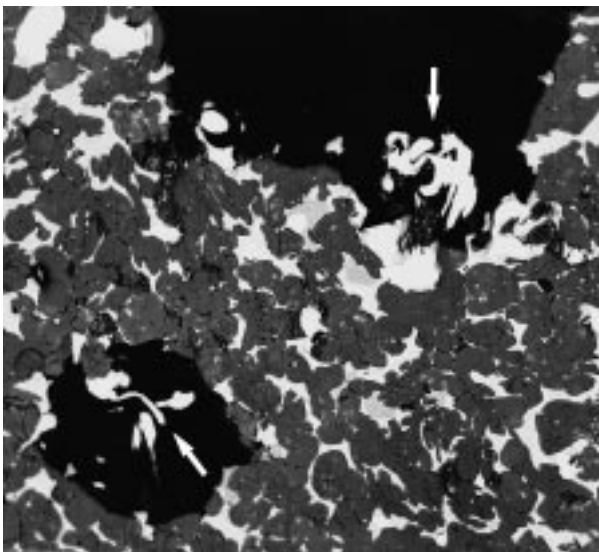

Figure 21. Microstructure of the oval cap shown in Figure 20. Filament copper has grown into pores at the bottom of the cap, where it merges with the main cake. Magnification 20. As polished.

Figure 22. Microstructure of Type I metal prill (3402): near-parallel laths of speiss (grey) in γ-Cu$_3$As matrix (pale grey), with bridging α-(Cu,As) phase (white). Dendritic matte grows from a surface rim into the metallic portion. Magnification 50. As polished.

also of temperature in the formation of bornite. At a given level of oxygen, bornite is more stable at low temperatures, hence it is more likely to be generated by the slower cooling rate of the furnace than by the more rapid cooling of the crucible. Carefully controlled experiments are required to make a more definitive thermodynamic description of these processes.

Figure 28 illustrates the chalcocite and bornite mattes in the ternary Cu–Fe–S diagram as part of the pseudo-binary Cu$_2$S–FeS system which has been described by many authors. Metallurgists distinguish among various mattes produced industrially: coarse (low-grade) matte contains more iron than copper; rich (high-grade) matte, more copper than iron. White metal is almost pure Cu$_2$S; blue metal contains about 62 weight% Cu, and "pimpled metal" has precipitated

metallic copper. The definition of "blue metal" is the best match for matte product 3396, given its metallographic description (exhibiting various shades of blue) and its composition (58·4 weight% Cu; see Table 6).

Matte copper (filament copper)

Pure copper formed only in bornite mattes that issued from the furnace smelts. It grew into surface pores or fissures in these mattes or appeared as a band at the interface of matte and metal alloy. The miscibility gap in the Cu–Fe–S system (see Figure 28) accounts for this effect (Tiedemann, 1926; Tafel, 1951). Pure copper forms from a melt with the approximate composition (Cu$_2$S)$_2$FeS (≈ 62 weight% Cu). The melt decomposes to bornite, and copper precipitates as "capillary copper" or "filament copper". Tiedemann (1926) defines the reaction as:

$$4(Cu_2S)_2FeS \rightarrow 2 \ (Cu_2S)_3Fe_2S_3 + 4 \ Cu$$
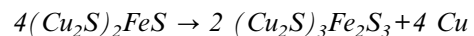
The melt has to be rich in Cu$_2$S for the reaction to take place (Tafel, 1951) because it is the Cu$_2$S that partially reacts:

$$Cu_5FeS_4 \rightarrow 2 \ Cu_2S \cdot CuS \cdot FeS$$
$$\text{and}$$
$$Cu_2S \rightarrow CuS + Cu$$
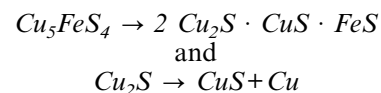
The maximum extent of copper precipitation takes place in a melt with ≈ 62 weight% Cu. At this composition, up to 15·7% of the melt, or 25% of the melt's copper can precipitate as filament copper. Reaction
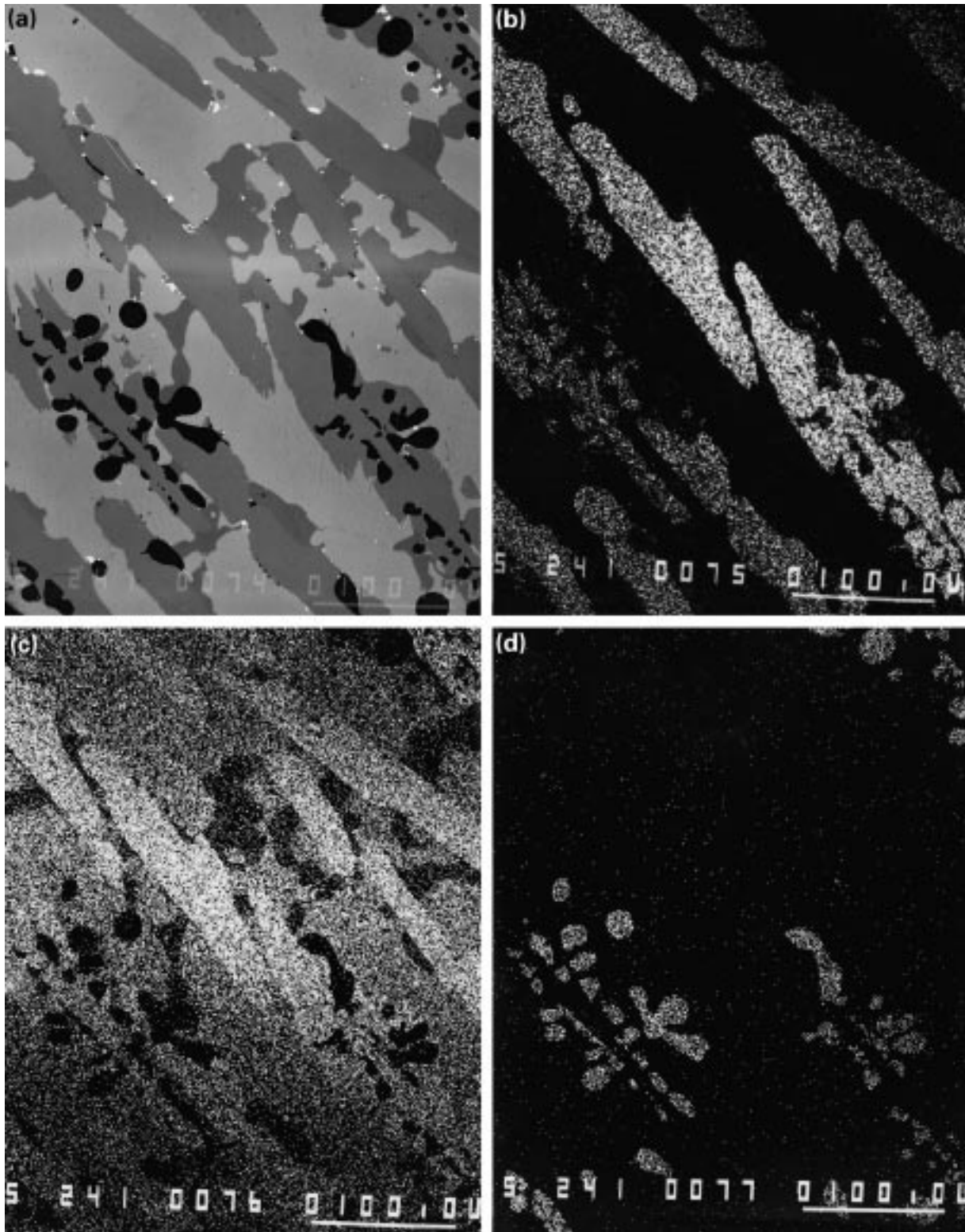
Figure 23. (a) Backscattered electron image of Type I prill (3402), with parallel speiss laths (dark grey) and matte dendrites (black). Bismuth-rich inclusions (white) concentrate at interfaces between speiss and the γ-Cu$_3$As matrix (light grey). (b) X-ray image for Fe $K\alpha$ showing the iron–rich speiss phase illustrated in (a). (c) X-ray image for As $L\alpha$. Note that the highest concentration of arsenic occurs in the speiss laths, but the γ-Cu$_3$As matrix is also arsenic rich. (d) X-ray image for S $K\alpha$ highlighting the sulphur-rich matte dendrites of (a). Magnification 240 for each.
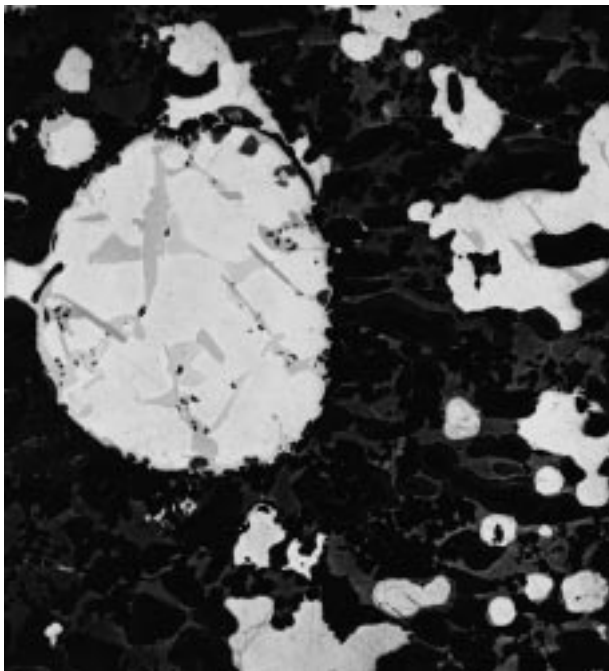
Figure 24. Microstructure of Type II metal prill (3402): the primary α-(Cu,As) phase (white) is surrounded by interdendritic γ-Cu₃As material (pale grey); laths and irregularly shaped speiss phases (darker grey) and matte inclusions (black) occur throughout the section. The surrounding material contains cored grains of calcium sulphate. Magnification 100. As polished.

temperatures are between 548° and 180°C (Tiedemann, 1926). The matte compositions produced in the two furnace cosmelting experiments fall between 58·4 weight% Cu (3396: chemical analysis) and 69 weight% Cu (3402: WDS electron microanalysis). Referring to Figure 28, these matte products lie close to the upper corner of the miscibility gap where copper precipitation from the melt is at a maximum. It is clear why so much pure copper precipitated into pores, fissures, and formed as a relatively broad band (3396) in the furnace bornite mattes.

Speiss formation
Speisses are unwelcomed by-products of copper smelting. They include primarily a wide variety of arsenides and antimonides. In the experiments reported here, we have identified copper–iron arsenides in the furnace products of cosmelts 3396 and 3402. Matte can dissolve arsenic, but arsenic solubility in matte decreases as the copper content rises. This situation can lead to the formation of speiss phases within the matte. The formation of speiss depends even more upon the concentration of iron in the system, since iron has a higher affinity for arsenic than copper has (Kleinheisterkamp, 1948). Speiss can distribute within matte only to a limited extent (see Figure 15). If the matte becomes saturated with speiss, any speiss above the solubility limit is rejected and enters the alloy (Tafel, 1951). This

occurred in furnace cosmelting products 3396 and 3402. In both cases, some arsenides are present in the alloy: the ingot (3396) and the Type II prills (3402) (see Table 8 & Table 10). The phase diagram in Figure 29 shows the zones in which arsenide and antimonide speisses form in the ternary Cu–Fe–As system. We have plotted on the diagram the location of the speisses identified in furnace products 3396 and 3402.

Slag
Glassy slag formed in only one of the four experiments: the furnace cosmelt with oxide and enargite (3396). In the comparable furnace experiment with arsenopyrite (3402), Table 5 indicates that the constituents of the charge might have been self-fluxing: 7·6 weight% Fe, 10·7% SiO_2, and 11·1% CaO; no glassy slag formed. The corresponding elemental concentrations in furnace charge 3396 were: 13·4 weight% Fe, 13·4% SiO_2, and only 2·3% CaO, but the 3396 cosmelt produced a thick slag layer. Both smelts ran for approximately the same duration (50 min; see Figure 3). The furnace temperature in the arsenopyrite experiment never exceeded 1000°C. During the final 25 min of the enargite experiment, the furnace temperature rose from 1000°, peaked at ≈ 1180°, then dropped to 1100°C. In addition, the fuel ash contributed major amounts of CaO to the gangue, as analysis of the 3396 slag shows (see Table 6). These results demonstrate that low concentrations of Fe and SiO_2 in a furnace charge can produce glassy slags in a self-fluxing system if the furnace temperature is high enough and if other materials, such as ash, also act to flux the gangue. A temperature of 1150°–1200°C is not difficult to achieve in a forced draught, bowl furnace.

Referring to the temperature versus time plots in Figure 3, we would not expect glassy slag to have formed in crucible experiments 3389 (enargite) or 3391 (arsenopyrite). Neither charge contained sufficient Fe, SiO_2, and CaO to be self-fluxing at the operating temperatures shown in Figure 3. The surprising result of these two crucible cosmelts is that the granular and crusty materials that surround the alloy ingots are similar in composition, in spite of the considerable differences in the charges. Both cosmelts produced large volumes of CuCl (nantokite), the matrix material, interspersed with a variety of sulphides and oxides of copper and iron. The granular texture of the enargite product (3389) resulted from an abundance of SiO_2 grains; the arsenopyrite product was far denser.

Significance of Results for Archaeology

Whether or not cosmelting procedures were responsible for the production of copper–arsenic alloys at certain times and places in prehistory can be determined only by investigation of the production sites themselves. In the case of Batán Grande, the exper-
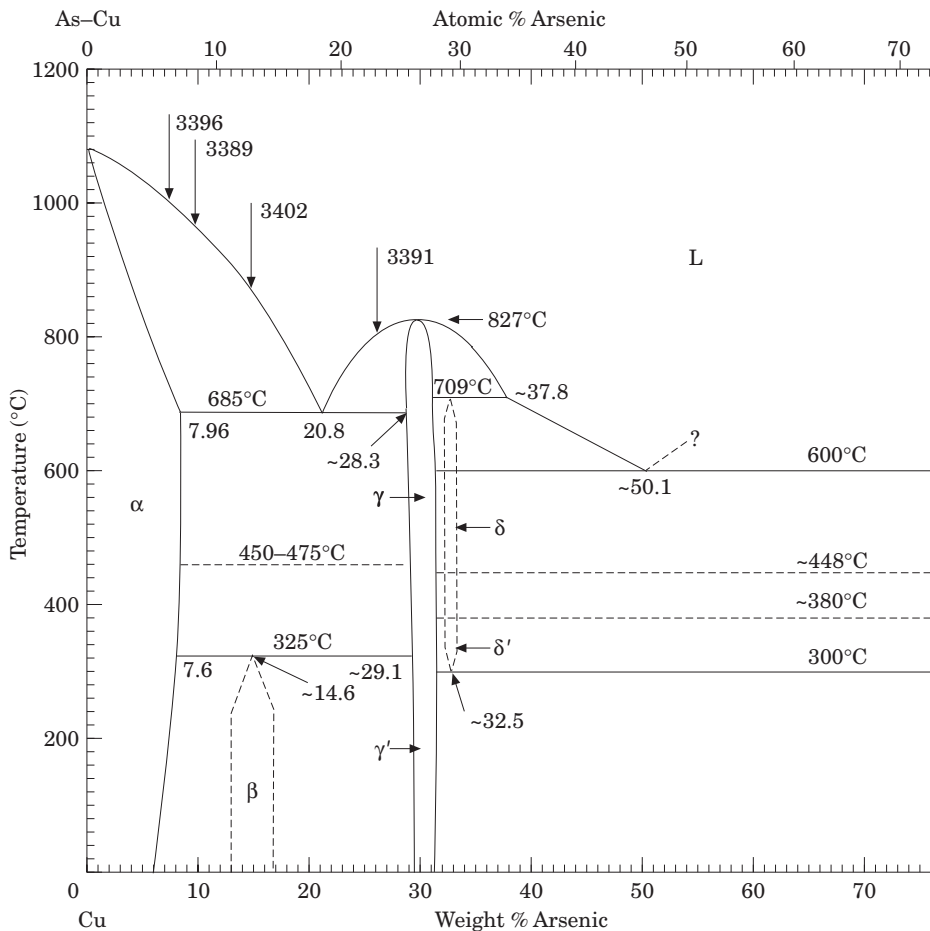
Figure 25. Binary phase diagram of the As-Cu system showing the bulk compositions of cosmelting product alloys 3389, 3391, 3396, and 3402 (estimated value).

imental results reported here (especially experiment 3402) coincide closely with reconstructions of furnace smelting operations suggested by the archaeological data. Our study demonstrates that cosmelting is a straightforward and simple technology, relying on a set of procedures that departs only slightly, if at all, from those metalworkers had developed for the direct reduction smelting of oxide ores. Oxide ores of copper often contain some of the primary sulphides from which the oxides formed. Unless miners deliberately discarded the blue-to-black coloured sulphides when comminuting their ores, the crucible or furnace charge would have often contained a natural mixture of oxides and sulphides, or sulpharsenides. Our experiments show that such cosmelts produce clean, coherent metal or alloy ingots over a wide range of oxide-to-sulphide ratios, even when the sulphide component is as rich as in a 2:1, oxide: sulphide charge. Given the length of time during which copper–arsenic alloys were produced in the Old World, over vast geographical regions from the Near East to western Europe and Britain, it seems reasonable to consider that cosmelting naturally mixed charges accounted for much of this production.

Appreciation of the feasibility of cosmelting processes and the likelihood of their widespread utilization over several millennia should lead archaeologists to re-examine some long-held opinions about the development of metallurgy, especially in the Old World. The fact that sulphide ores cannot be reduced by carbon monoxide in a direct smelting process, in the same way that oxide ores can be reduced, prompted explanations that are generally accepted about how early metalworkers exploited sulphide ores in order to win copper or arsenical copper alloys from them. These explanations suggest that (1) sulphide ores were roasted to drive off sulphur and to oxidize copper so that the oxidized ore could be direct smelted with charcoal; or (2) the sulphide ore was partially roasted and oxidized, then smelted to form some metal and matte; the matte was further roasted to oxide and, ultimately, reduction smelted. Both methods represent extractive metallurgical practice modern industry has used until recently for smelting sulphide ores!

During the period with which archaeology is concerned, however, whenever the sulphide ore was a sulpharsenide, the consequence to local communities of the ore roasting step would have been the emission
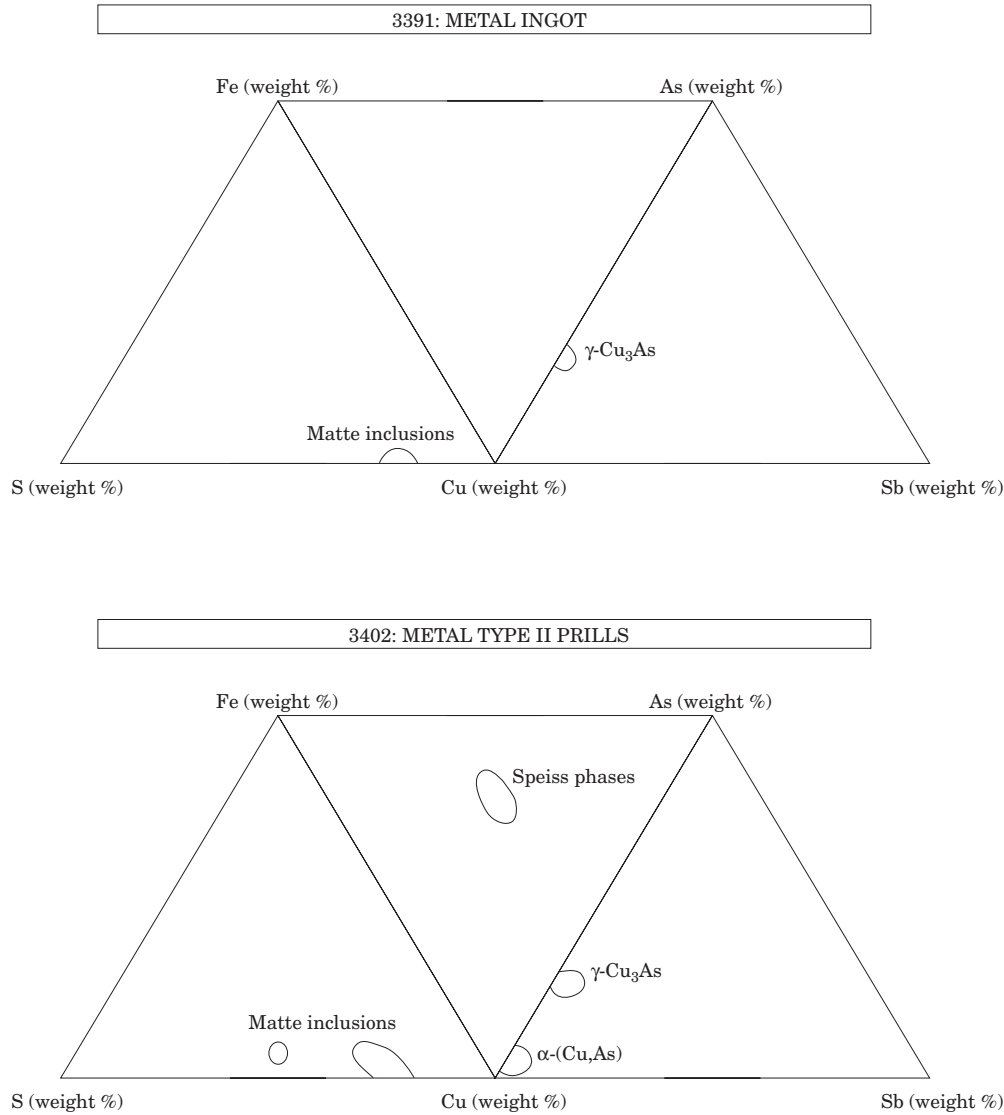
Figure 26. Combined ternary diagrams (As–Cu–Fe–S–Sb) showing the major components of metal ingot product 3391 and metal Type II prill product 3402.

of considerable quantities of arsenious oxide to the environment, with possible long-term hazardous health effects. Many Old World archaeologists have argued (see Lechtman, 1996) that one of the primary reasons for which tin bronze ultimately replaced arsenic bronze was precisely because of the environmental consequences attending release of noxious arsenic oxide fumes. Cosmelting copper oxide ores with copper or iron sulpharsenide ores dramatically lessens this problem. The ore roasting step is unnecessary. Closed-crucible cosmelting virtually eliminates the generation of arsenious oxide fume; furnace cosmelting reduces the emissions to manageable levels.

Archaeological documentation of cosmelting as a widespread metallurgical practice would call into question not only the argument that arsenic bronze production was abandoned in the Old World because of

environmental pollution. It will also call for archaeologists to reassess claims that the invasion by miners of the sulphide, or primary ore zone required development of revolutionary new techniques for dealing with an intractable material resource. Suddenly metalworkers had to invent roasting, matte handling, and smelting techniques that bore little relation to traditions of reduction smelting. Several scholars (see, e.g., Charles, 1980; Rostoker & Dvorak, 1991) have pointed out that, on the contrary, experience with sulphide ores was likely achieved much more gradually and related to the practice of cosmelting. By the time miners had exhausted rich and readily accessible oxide ore zones they already had considerable experience dealing with sulphides present in the same deposits.

The Americas provide the best evidence thus far not only for cosmelting to produce arsenic bronze but for

Table 11. Principal input and product components of the four cosmelting experiments

|	Crucible/furnace charge			Smelting products
	Principal Cu and As ore minerals	+	Principal associated minerals and intermediate reaction products	Principal product components
Cosmelting experiments with enargite				
Crucible cosmelting (product MIT 3389):	$Cu_7Cl_4(OH)_4 \cdot H_2O + Cu_3AsS_4$	+	$CuCl + SiO_2$	α-(Cu,As)+ $\sim Cu_2S + CuCl + SiO_2 + Ca_3(SO_3)_2SO_4$
Furnace cosmelting (product MIT 3396):	$Cu_7Cl_4(OH)_4 \cdot H_2O + Cu_3AsS_4$	+	$SiO_2 + FeO$	α-(Cu,As)+$Cu_5FeS_4 + Fe_2SiO_4$
Cosmelting experiments with arsenopyrite				
Crucible cosmelting (product MIT 3391):	$Cu_7Cl_4(OH)_4 \cdot H_2O + FeAsS$	+	$CuCl + SiO_2$	γ-$Cu_3As+ \sim Cu_2S + FeS + Fe_3O_4 + SiO_2 + CuCl$
Furnace cosmelting (product MIT 3402):	$Cu_7Cl_4(OH)_4 \cdot H_2O + FeAsS$	+	$SiO_2 + CaO + MgO$	α-(Cu,As)+$Cu_5FeS_4 + \beta$-$Ca_2SiO_4 + Ca(Fe,Mg)SiO_4$
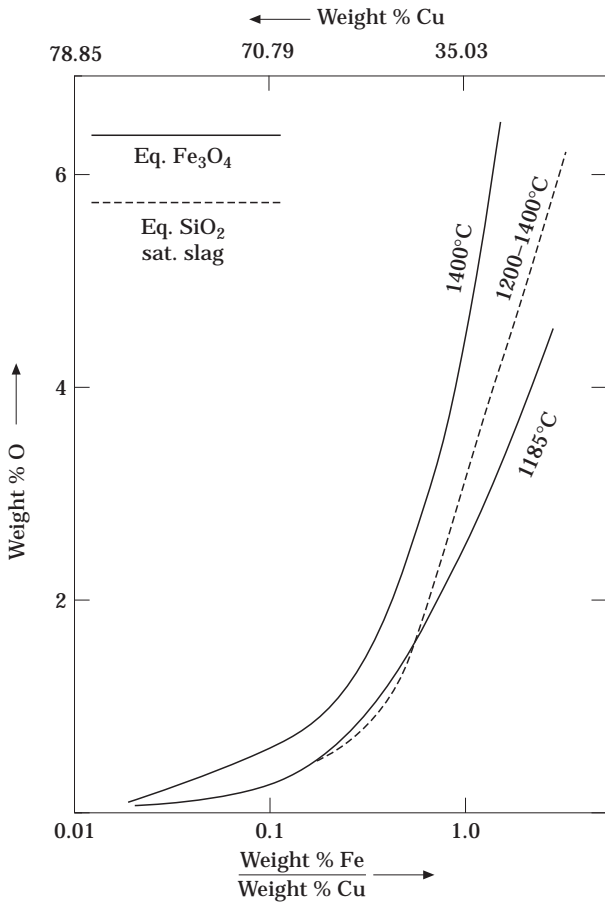
Figure 27. Solubility of oxygen in copper mattes as a function of the iron to copper ratio and at different temperatures. The iron to copper ratios are converted to copper concentrations on the assumption that the matte consists of a binary mixture of Cu_2S and $FeS_{1.05}$ (from Rosenqvist, 1983: figure 12–4(b), after Kuxmann & Bor, 1965: figure 4).

Figure 28. Ternary phase diagram for the system Cu–Fe–S, indicating the region of matte decomposition and copper precipitation for temperatures between 548° and 180°C (after Tiedemann, 1926). The cosmelted bornite mattes of experiments 3396 and 3402 are located on the diagram.

Figure 29. Ternary phase diagram for the As–Cu–Fe system, locating the regions of metallurgical speiss compositions (after Kleinheisterkamp, 1948). The speiss compositions of the experimental cosmelting products fall within these fields.

the deliberate addition of arsenic-bearing ores to a charge of copper oxides. Copper mines in the near vicinity of Batán Grande, Peru, known to have been exploited in prehistory, provided the copper oxide ores smelted at the site. None of these deposits contains arsenic minerals. There is no doubt that arsenic-bearing minerals were deliberately added to the furnace charges to yield the copper–arsenic alloys that were Batán Grande's primary product for many centuries. The nearby Cerro Mellizo mine, located south of Batán Grande, has abundant arsenopyrite and scorodite ($FeAsO_4 \cdot 2H_2O$) mineralization and is believed by the excavators to have served as the source of the arsenic ore cosmelted in the furnaces (Merkel et al., 1994).

In west Mexico, Hosler (1988, 1994) argues that arsenopyrite was the primary source of arsenic there for the extensive production of arsenic bronze from about CE 1200 to the European invasion. Some of the west Mexican arsenic bronze cast bells she analysed contain more than 13 weight% arsenic, including
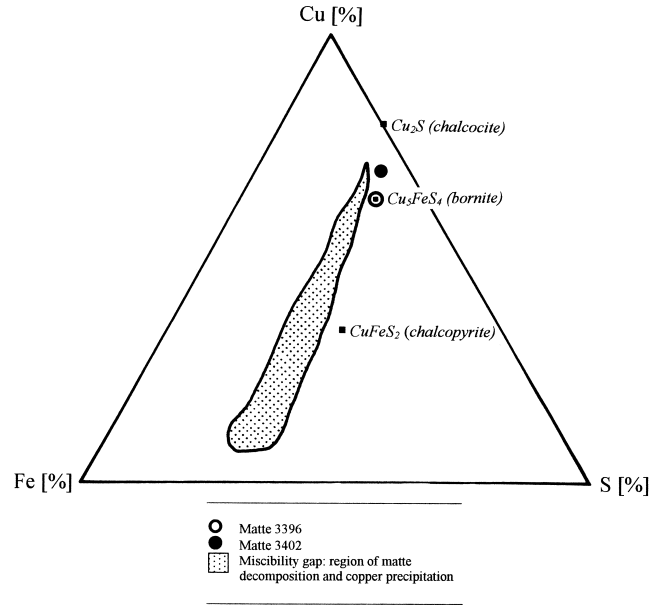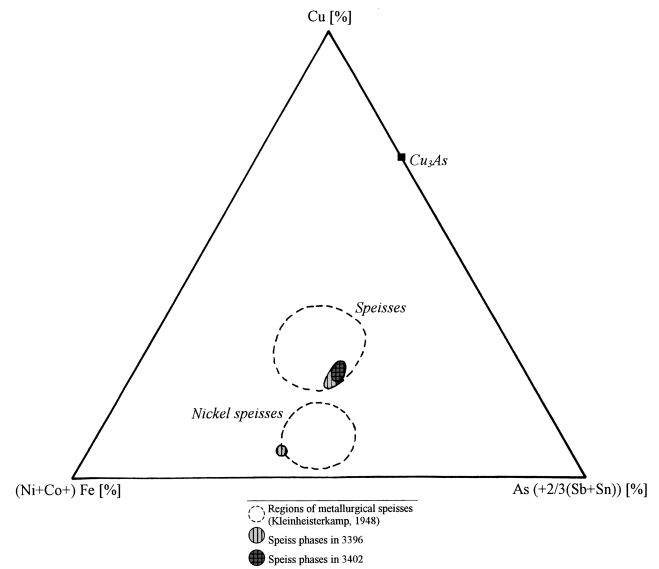
several with an arsenic concentration of between 22 and 23% (Hosler, 1994: appendix A2·1). Support for Hosler's contention that these high-arsenic alloys were likely made by cosmelting oxide ores of copper with arsenopyrite is provided by our crucible cosmelting experiments with arsenopyrite (3391) which produced bronzes containing 26 weight% arsenic.

The experimental results reported here indicate that cosmelting achieves excellent results whether the sulpharsenides are ores of copper or of iron. Charges may be natural ore mixtures or deliberate mixtures. The sulpharsenides may be primary ores or partially weathered ores. The technology is successful because it provides useful results over a wide range of operating conditions. We need new archaeological field investigations of smelting and processing sites to determine the temporal and geographical extent of this extractive metallurgical regime.

Acknowledgements

References

Charles, J. A. (1979). From copper to iron—the origin of metallic materials. *Journal of Metals* **31,** 8–13.

Charles, J. A. (1980). The coming of copper and copper-base alloys and iron: a metallurgical sequence. In (T. A. Wertime & J. D. Muhly, Eds) *The Coming of the Age of Iron.* New Haven, CT: Yale University Press, pp. 151–181.

Epstein, S. M. (1993). *Cultural choice and technological consequences: constraint of innovation in the late prehistoric copper smelting industry of Cerro Huaringa, Peru.* Ph.D. Thesis. University of Pennsylvania.

Epstein, S. M. & Shimada, I. (1983). Metalurgia de Sicán. Una reconstrucción de la producción de la aleación de cobre en el Cerro de los Cementerios, Perú. *AVA-Beiträge* **5,** 379–430.

Heskel, D. & Lamberg-Karlovsky, C. C. (1980). An alternative sequence for the development of metallurgy: Tepe Yahya, Iran. In (T. A. Wertime & J. D. Muhly, Eds) *The Coming of the Age of Iron.* New Haven, CT: Yale University Press, pp. 229–265.

Hosler, D. (1988). The metallurgy of ancient west Mexico. In (R. Maddin, Ed.) *The Beginning of the Use of Metals and Alloys.* Cambridge, MA: MIT Press, pp. 328–343.

Hosler, D. (1994). *The Sounds and Colors of Power: The Sacred Metallurgical Technology of Ancient West Mexico.* Cambridge, MA: MIT Press.

Kleinheisterkamp, H. (1948). Einige grundlegende Gleichgewichte bei der Bildung metallurgischer Speisen. *Erzmetall* **1,** 65–96.

Kuxmann, U. & Bor, F. Y. (1965). Untersuchungen zur Löslichkeit von Sauerstoff in Kupfersteinen unter kieselsäuregesättigten Eisenoxidschlacken. *Erzmetall* **18,** 441–450.

Lechtman, H. (1976). A metallurgical site survey in the Peruvian Andes. *Journal of Field Archaeology* **3,** 1–42.

Lechtman, H. (1979). Issues in Andean metallurgy. In (E. P. Benson, Ed.) *Pre-Columbian Metallurgy of South America.* Washington, D.C.: Dumbarton Oaks, pp. 1–40.

Lechtman, H. (1985). The manufacture of copper–arsenic alloys in prehistory. *Journal of the Historical Metallurgy Society* **19,** 141–142.

Lechtman, H. (1996). Arsenic bronze: dirty copper or chosen alloy? A view from the Americas. *Journal of Field Archaeology* **23,** 477–514.

Lechtman, H. (1997). El bronce arsenical y el Horizonte Medio. In (R. Varón G. & J. Flores E., Eds) *Arqueología, Antropología e Historia en los Andes.* Lima: Instituto de Estudios Peruanos, pp. 153–186.

Lorenzen, W. (1965). *Helgoland und das früheste Kupfer des Nordens.* Otterndorf: Otterndorfer Verlagsdruckerei.

Merkel, J. & Shimada, I. (1988). Arsenical copper smelting at Batán Grande, Peru. *IAMS Newsletter* **12,** 4–7.

Merkel, J. F., Shimada, I., Swann, C. P. & Doonan, R. (1994). Pre-hispanic copper alloy production at Batán Grande, Peru: interpretation of the analytical data for ore samples. In (D. A. Scott & P. Meyers, Eds) *Archaeometry of Pre-Columbian Sites and Artifacts.* Los Angeles, CA: The Getty Conservation Institute, pp. 199–227.

Muhly, J. D. (1988). The beginnings of metallurgy in the Old World. In (R. Maddin, Ed.) *The Beginning of the Use of Metals and Alloys.* Cambridge, MA: MIT Press, pp. 2–20.

Pazuchin, V. A. (1964). On the origin of ancient copper containing arsenic. *Izvestia Akademii Nauk SSSR—Metallurgia i Gornoe Delo* **1,** 151–165.

Rapp Jr., G. (1989). Determining the origins of sulfide smelting. In (A. Hauptmann, E. Pernicka & G. A. Wagner, Eds) *Old World Archaeometallurgy.* Bochum: Selbstverlag des Deutschen Bergbau-Museums, pp. 107–110.

Rehder, J. E. (1994). Blowpipes versus bellows in ancient metallurgy. *Journal of Field Archaeology* **21,** 345–350.

Rosenqvist, T. (1983). *Principles of Extractive Metallurgy.* New York: McGraw-Hill.

Rostoker, W. & Dvorak, J. R. (1991). Some experiments with co-smelting to copper alloys. *Archaeomaterials* **5,** 5–20.

Rostoker, W., Pigott, V. C. & Dvorak, J. R. (1989). Direct reduction to copper metal by oxide-sulfide mineral interaction. *Archaeomaterials* **3,** 69–87.

Schubert, K., Breimer, H., Burkhardt, W., Günzel, E., Haufler, R., Lukas, H. L., Vetter, H., Wegst, J. & Wilkens, M. (1957). Einige strukturelle ergebnisse an metallischen phasen II. *Die Naturwissenschaften* **44,** 229–230.

Shimada, I., Epstein, S. M. & Craig, A. K. (1982). Batán Grande: a prehistoric metallurgical center in Peru. *Science* **216,** 952–959.

Shimada, I. & Merkel, J. F. (1991). Copper-alloy metallurgy in ancient Peru. *Scientific American* **265,** 80–86.

Sundman, B., Jansson, B. & Anderson, J.-O. (1985). The Thermo-Calc data base system. *Calphad* **9,** 153–190.

Tafel, V. (1951). *Lehrbuch der Metallhüttenkunde.* Bd. 1 Leipzig: S. Hirzel Verlagsbuchhandlung.

Tiedemann, H. (1926). Die Haarkupferbildung im Kupferstein. *Metall und Erz* **23,** 200–210.

Tylecote, R. F. (1980a). Furnaces, crucibles, and slags. In (W. A. Wertime & J. D. Muhly, Eds) *The Coming of the Age of Iron.* New Haven, CT: Yale University Press, pp. 183–227.

Tylecote, R. F. (1980b). Summary of results of experimental work on early copper smelting. In (W. A. Oddy, Ed.) *Aspects of Early Metallurgy.* London: British Museum, pp. 5–12.

Tylecote, R. F., Ghaznavi, H. A. & Boydell, P. J. (1977). Partitioning of trace elements between the ores, fluxes, slags and metal during the smelting of copper. *Journal of Archaeological Science* **4,** 305–333.

Vidal, C. E. (1985). Metallogenesis associated with the coastal batholith of Perú: a review. In (W. S. Pitcher, M. P. Atherton, E. J. Cobbing & R. D. Beckinsale, Eds) *Magmatism at a Plate Edge—the Peruvian Andes.* Glasgow: Blackie, pp. 243–249.

Zwicker, U., Greiner, H., Hofmann, K.-H. & Reithinger, M. (1985). Smelting, refining, and alloying of copper and copper alloys in crucible furnaces during prehistoric up to Roman times. In (P. T. Craddock & M. J. Hughes, Eds) *Furnaces and Smelting Technology in Antiquity.* London: British Museum, pp. 103–115.